SCATTERING FROM IMPEDANCE OBJECTS AT THE EDGE OF A PERFECTLY CONDUCTING WEDGE

A THESIS

SUBMITTED TO THE DEPARTMENT OF ELECTRICAL AND

ELECTRONICS ENGINEERING

AND THE GRADUATE SCHOOL OF ENGINEERING AND SCIENCE

OF BILKENT UNIVERSITY

IN PARTIAL FULFILLMENT OF THE REQUIREMENTS

FOR THE DEGREE OF

MASTER OF SCIENCE

By

Behnam Ghassemiparvin

September, 2012

I certify that I have read this thesis and that in my opinion it is fully adequate, in scope and in quality, as a thesis for the degree of Master of Science.

Prof. Dr. Ayhan Altıntaş(Advisor)

I certify that I have read this thesis and that in my opinion it is fully adequate, in scope and in quality, as a thesis for the degree of Master of Science.

Assoc. Prof. Dr. Vakur B. Ertürk

I certify that I have read this thesis and that in my opinion it is fully adequate, in scope and in quality, as a thesis for the degree of Master of Science.

Prof. Dr. Özlem Aydın Çivi

Approved for the Graduate School of Engineering and Science:

Prof. Dr. Levent Onural
Director of the Graduate School

ABSTRACT

SCATTERING FROM IMPEDANCE OBJECTS AT THE EDGE OF A PERFECTLY CONDUCTING WEDGE

Behnam Ghassemiparvin
M.S. in Electrical and Electronics Engineering
Supervisor: Prof. Dr. Ayhan Altıntaş
September, 2012

In this study, scattering from impedance bodies positioned at the edge of a perfectly conducting (PEC) wedge is investigated. In the treatment of the problem, eigenfunction expansion in terms of spherical vector wave functions is employed. A complete dyadic Green's function for the spherical impedance boss at the edge is developed and through decomposing the dyadic Green's function, it can be observed that the contribution of the scatterer is separated from the wedge. It is shown that the scattering is highly enhanced by the edge guided waves. For the general case of irregularly shaped scatterer the solution is extended using T-matrix method. The method is implemented by replacing free space Green's function with the dyadic Green's function of the PEC wedge. The solution is verified by applying it to the case of spherical scatterer and results are compared with the dyadic Green's function solution. The T-matrix solution is generalized for the multiple scatterer case. Numerical results are obtained for two impedance scatterers at the edge and compared with the PEC case.

Keywords: Electromagnetic scattering, eigenfunction expansion, spherical vector wave functions, dyadic Green's function, T-matrix.

ÖZET

MÜKEMMEL İLETKEN BİR KAMA ÜZERİNDEKİ EMPEDANS CİSİMLERDEN SAÇILMA

Behnam Ghassemiparvin
Elektrik ve Elektronik Mühendisliği, Yüksek Lisans
Tez Yöneticisi: Prof. Dr. Ayhan Altıntaş
Eylül, 2012

Bu çalışmada mükemmel iletken bir kama üzerindeki empedans cisimlerden saçılma problemi araştırılmıştır. Bu problemin çözümünde küresel vektör dalga fonksiyonu kullanılarak özfonksiyon açılımı yapılmıştır. Kama üzerındeki küresel empedans cisim için tam bir diyadik Green fonksiyonu geliştirilmiş ve bu Green fonksiyonu bileşenlerine ayrılarak, saçıcının katkısının kamanınkinden ayrılabildiği gözlemlenmiştir. Saçılmanın kenar kılavuzlu dalgalarla büyük ölçüde güçlendiği gösterilmiştir. Çözüm, düzensiz şekle sahip olan bir saçıcı için, T-matris yöntemi kullanılarak genelleştirilmiştir. T-matris yöntemini uygulamak için, serbest uzay Green fonksiyonunun yerine, mükemmel iletken kamanın diyadik Green fonksiyonu kullanılmıştır. T-matris yöntemi, küresel saçıcı problemine uygulanmış ve sonuçlar diyadik Green fonksiyonu ile karşılaştırılarak doğrulanmıştır. T-matris çözümü çoklu saçıcı problemi için genellenmiştir. Kenar üzerindeki iki empedans cisim için sayısal sonuçlar elde edilmiş ve mükemmel iletken cisimler için olan sonuçlarla karşılaştırılmıştır.

Anahtar sözcükler: Elektromanyetik saçılma, özfonksiyon açılımı, küresel vektör dalga fonksiyonu, diyadik Green fonksiyonu, T-matris.

Acknowledgement

I would like to express my sincere gratitude to Prof. Dr. Ayhan Altıntaş for his supervision, guidance and the suggestions throughout the development of this thesis. It was an honor for me to work with him and benefit from his deep knowledge and experience in electromagnetics.

I also wish to thank Prof. Dr. Özlem Aydın Çivi and Assoc. Prof. Dr. Vakur B. Ertürk for evaluating and commenting on my thesis as a jury member.

I also like to thank Volkan Açikel and Ramez Kian for their support, friendship and invaluable suggestions in the preparation of this thesis.

Finally, I am deeply indebted to Aslı Ünlügedik for her friendship and encouragement. I am also grateful for her ingenious suggestions and honest criticism on my work.

Contents

List of Figures

List of Tables

Chapter 1

Introduction

In this study, we investigate the scattering from impedance objects at the edge of a perfectly conducting (PEC) wedge and effects of the scatterers and their interaction with the wedge is analyzed. Both the wedge geometry and scatterers on the edge are encountered in a variety of engineering problems. Specially in wireless communications, developing accurate propagation models plays a key role in network planning. Furthermore, wedge-like structures and objects on edge are highly involved in modeling of radar targets. Analytical treatment of such canonical structures provide accurate and fast simulations and also give physical insight of the problem.

In the literature, the problem of cylinder-tipped half plane is first considered by Keller which Geometrical Theory of Diffraction (GTD) solution is presented [1]. Shortcomings of the Keller's theory in the shadow regions were overcome by incorporating the higher order terms in the solution, hence, continuous fields at the boundaries are obtained [2]. For the general case of cylinder-tipped wedge, using GTD approach, an asymptotic expression of Green's function is obtained in [3]. Also in [4], Green's function of a cylinder-tipped wedge with a sectoral groove is determined using cylindrical vector wave functions. For the cases of grooved wedge [5] and the wedge truncated close to the edge [6], based on application of equivalence principle, the problem is divided into distinct exterior and interior problems. Exterior problem is concerned with wedge scattering

which is formulated using UTD or Green's function expansion. Interior problem of cavity is treated by employing finite element method. Nevertheless, published works mostly refer to configurations which conform to cylindrical coordinates and do not consider the scattering from structures at the edge. However, scattering from perfectly conducting objects near the edge is considered in [7] where spherical vector wave functions are employed in order to achieve accurate results near the edge.

In this work, we will develop a general solution for the scattering from spherical and irregularly-shaped impedance objects at the edge. An important aspect of the problem is the effect of edge guided waves on the scattered field from the objects and their interactions with each other. In order to accurately analyze the region near the edge and also three dimensional geometry of the problem, eigenfunction expansion technique in terms of spherical vector wave functions is employed.

Initially, a dyadic Green's function for a spherical impedance boss will be developed which is the exact solution and will be used to compare with the numerical results. Effects of the boss and its mutual interaction with the wedge will be isolated by decomposing the Green's function.

T-matrix method will be used for the case of irregularly shaped scatterers. To facilitate the implementation of the T-matrix, conventional formulation will be modified by replacing the free space Green's function with the Green's function of the wedge. T-matrix solution will be verified by comparing the results of the dyadic Green's function for the spherical boss. T-matrix method is then used to treat the problem of multiple scatterers at the edge where mutual effect of the scatterers is considered.

In Chapter 2, we present complete dyadic Green's function for a spherical impedance boss at the edge . General case of an irregularly-shaped scatterer at the edge is considered in Chapter 3 and the numerical solution using T-matrix method is provided. In Chapter 4, T-matrix solution is first extended for two scatterers then it is generalized for multiple objects. Numerical results for each case is presented and compared with the case of perfectly conducting objects

presented in [7]. Concluding remarks and future works are discussed in Chapter 5.

Through out this thesis $e^{j\omega t}$ time convention is assumed and suppressed. Normal vectors are assumed to be directing inside the volume. Electric and magnetic field intensities are denoted as $\bar{E}$ and $\bar{H}$, respectively.

Chapter 2

SPHERICAL IMPEDANCE BOSS AT THE EDGE

This chapter is mainly focused on the development of a complete dyadic Green's function of a spherical impedance scatterer at the edge of a perfectly conducting wedge. Full wave analysis of the problem based on the eigenfunction expansion is carried out. Since scattering from objects at the edge is of interest, a three-dimensional Green's function is formulated in terms of spherical vector wave functions. Initially, the relation between dyadic Green's function and electric field intensity will be established. Then an incomplete dyadic Green's function is introduced which is valid in the source free region. Finally, in order to obtain a valid solution in the source region, general source correction term introduced by Pahthak [8] is added. It is observed that total field can be represented by the sum of two terms: total field in the presence of the wedge with scatterer removed and the scattered field from the impedance boss and its interaction with the wedge.

2.1 Relationship Between Electric Field and Dyadic Green's Function

First step in the treatment of the problem is to define electric field intensity in terms of the dyadic Green's function. In this process, differential equations and boundary conditions that should be satisfied by the electric field and the dyadic Green's function are determined. Then, by employing Green's second identity desired relationship between electric field and dyadic Green's function will be obtained.

Geometry of the problem is shown in Fig. 2.1. A perfect electrically conducting (PEC) wedge with exterior angle γ is considered which extends infinitely in the z direction. One side of the wedge lies on the xz plane. A spherical impedance boss with radius a is centered at the edge of the PEC wedge. Position vectors, $\bar{R} = r\hat{r}$ and $\bar{R}' = r'\hat{r}'$, denote the observation and the source locations, respectively. S_W and S_B denotes the surface of the wedge and the boss, respectively, and Σ is an imaginary spherical surface which extends to infinity. These surfaces enclose the volume V and $\hat{n}$ is the unit normal vector directed into the volume.

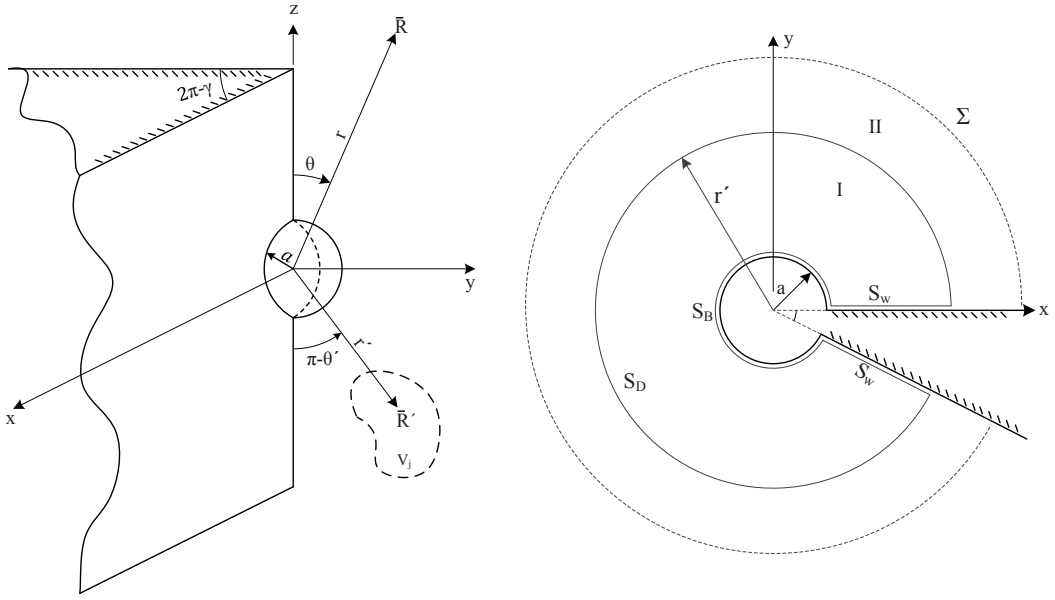

Figure 2.1: Geometry of the spherical boss placed at the edge of a wedge

The electric field intensity, $\bar{E}(\bar{R})$, due to the volume current density,$\bar{J}_v(\bar{R})$, which is confined to volume V_j, must satisfy the vector differential equation in V.

$$\nabla \times \nabla \times \bar{E}(\bar{R}) - k_0^2 \bar{E}(\bar{R}) = -jk_0 Z_0 \bar{J}_v(\bar{R}) \tag{2.1}$$

where k_0 and Z_0 are the wave number and characteristic impedance of free space, respectively. In addition to Eq. (2.1), electric field should also satisfy the following boundary condition on the faces of the wedge, S_W,

$$\hat{n} \times \bar{E}(\bar{R}) = 0 \tag{2.2}$$

and also satisfies the standard impedance boundary condition [9] at surface of the boss, S_B,

$$\hat{n} \times \hat{n} \times \bar{E}(\bar{R}) = -\eta \hat{n} \times \bar{H}(\bar{R}) \tag{2.3}$$

where η is the surface impedance of the boss. Using the Maxwell's equation for source free region Eq. (2.3) can be written as

$$\hat{n} \times \hat{n} \times \bar{E}(\bar{R}) = \kappa \hat{n} \times \nabla \times \bar{E}(\bar{R}) \tag{2.4}$$

where

$$\kappa = \frac{\eta}{jk_0 Z_0}. \tag{2.5}$$

Dyadic Green's function of the wedge and the spherical impedance boss, $\bar{\bar{\Gamma}}_{WB}$, satisfies the following differential equation

$$\nabla \times \nabla \times \bar{\bar{\Gamma}}_{WB}(\bar{R}, \bar{R}') - k_0^2 \bar{\bar{\Gamma}}_{WB}(\bar{R}, \bar{R}') = -\bar{\bar{I}} \delta(\bar{R} - \bar{R}') \tag{2.6}$$

where $\bar{\bar{I}}$ is the unit dyad and $\delta(\bar{R} - \bar{R}')$ is the Dirac delta function. Boundary conditions satisfied by the electric field are imposed on the dyadic Green's function. Boundary condition at S_W is

$$\hat{n} \times \bar{\bar{\Gamma}}_{WB}(\bar{R}, \bar{R}') = 0. \tag{2.7}$$

and the impedance boundary condition at S_B can be written in terms of dyadic Green's function as follows

$$\hat{n} \times \hat{n} \times \bar{\bar{\Gamma}}_{WB}(\bar{R}, \bar{R}') = \kappa \hat{n} \times \nabla \times \bar{\bar{\Gamma}}_{WB}(\bar{R}, \bar{R}'). \tag{2.8}$$

Both electric field and the dyadic Green's function must satisfy the radiation condition on Σ and also the Meixner's edge condition [10] at the edge of the wedge.

In order to derive the relationship between $\bar{E}(\bar{R})$ and $\bar{\bar{\Gamma}}_{WB}(\bar{R},\bar{R}')$, Green's second identity for dyad and vector is applied as follows

$$\int_V \bar{E}(\bar{R}) \centerdot [\nabla\times\nabla\times\bar{\bar{\Gamma}}_{WB}(\bar{R},\bar{R}')] - [\nabla\times\nabla\times\bar{E}(\bar{R})] \centerdot \bar{\bar{\Gamma}}_{WB}(\bar{R},\bar{R}')\,\mathrm{dv}$$
$$= \int_{S_W+S_B+\Sigma} \{[\hat{n}\times\nabla\times\bar{E}(\bar{R})] \centerdot \bar{\bar{\Gamma}}_{WB}(\bar{R},\bar{R}') + [\hat{n}\times\bar{E}(\bar{R})] \centerdot [\nabla\times\bar{\bar{\Gamma}}_{WB}(\bar{R},\bar{R}')]\}\,\mathrm{ds}. \tag{2.9}$$

Using Eqs. (2.1) and (2.6) left hand side of the Eq. (2.9) can be simplified as

$$\int_V \{jk_0Z_0\bar{J}_v(\bar{R}) \centerdot \bar{\bar{\Gamma}}_{WB}(\bar{R},\bar{R}') - \bar{E}(\bar{R})\delta(\bar{R}-\bar{R}')\}\,\mathrm{dv}$$
$$= \int_{S_W+S_B+\Sigma} \{[\hat{n}\times\nabla\times\bar{E}(\bar{R})] \centerdot \bar{\bar{\Gamma}}_{WB}(\bar{R},\bar{R}') + [\hat{n}\times\bar{E}(\bar{R})] \centerdot [\nabla\times\bar{\bar{\Gamma}}_{WB}(\bar{R},\bar{R}')]\}\,\mathrm{ds} \tag{2.10}$$

If we consider the right hand side of the Eq. (2.9), integration on Σ will vanish because $\bar{E}(\bar{R})$ and $\bar{\bar{\Gamma}}_{WB}(\bar{R},\bar{R}')$ satisfy the radiation condition. Considering the boundary condition given in Eqs. (2.2) and (2.7) and using the vector identity,

$$[\hat{n}\times\nabla\times\bar{E}(\bar{R})] \centerdot \bar{\bar{\Gamma}}_{WB}(\bar{R},\bar{R}') = -[\nabla\times\bar{E}(\bar{R})] \centerdot [\hat{n}\times\bar{\bar{\Gamma}}_{WB}(\bar{R},\bar{R}')] \tag{2.11}$$

integration on S_W will also vanish. In order to derive the integration on S_B, boundary conditions given in Eqs. (2.4) and (2.8) are applied. Using the vector identity,

$$[\hat{n}\times\bar{E}(\bar{R})] \centerdot [\nabla\times\bar{\bar{\Gamma}}_{WB}(\bar{R},\bar{R}')] = -[\hat{n}\times\nabla\times\bar{\bar{\Gamma}}_{WB}(\bar{R},\bar{R}')] \centerdot \bar{E}(\bar{R}), \tag{2.12}$$

expression in Eq. (2.10) is simplified as

$$\int_{S_B} \{[\hat{n}\times\nabla\times\bar{E}(\bar{R})] \centerdot \bar{\bar{\Gamma}}_{WB}(\bar{R},\bar{R}') - [\hat{n}\times\nabla\times\bar{\bar{\Gamma}}_{WB}(\bar{R},\bar{R}')] \centerdot \bar{E}(\bar{R})\}\,\mathrm{ds}$$
$$= \int_{S_B} \frac{1}{\kappa}\{[\hat{n}\times\hat{n}\times\bar{E}(\bar{R})] \centerdot \bar{\bar{\Gamma}}_{WB}(\bar{R},\bar{R}') - [\hat{n}\times\hat{n}\times\bar{\bar{\Gamma}}_{WB}(\bar{R},\bar{R}')] \centerdot \bar{E}(\bar{R})\}\mathrm{ds}. \tag{2.13}$$

Using the vector identity,

$$[\hat{n} \times \hat{n} \times \bar{E}(\bar{R})] \cdot \bar{\bar{\Gamma}}_{WB}(\bar{R}, \bar{R}') = -[\hat{n} \times \bar{E}(\bar{R})] \cdot [\hat{n} \times \bar{\bar{\Gamma}}_{WB}(\bar{R}, \bar{R}')] \tag{2.14}$$

$$[\hat{n} \times \hat{n} \times \bar{\bar{\Gamma}}_{WB}(\bar{R}, \bar{R}')] \cdot \bar{E}(\bar{R}) = -[\hat{n} \times \bar{E}(\bar{R})] \cdot [\hat{n} \times \bar{\bar{\Gamma}}_{WB}(\bar{R}, \bar{R}')] \tag{2.15}$$

integration on S_B results in zero. Thus, the Eq. (2.9) reduces to

$$\int_V \bar{E}(\bar{R})\delta(\bar{R} - \bar{R}')\,\mathrm{dv} = jk_0 Z_0 \int_V J_v(\bar{R}) \cdot \bar{\bar{\Gamma}}_{WB}(\bar{R}, \bar{R}')\,\mathrm{dv} \tag{2.16}$$

which using the symmetry property of the dyadic Green's function,

$$\widetilde{\bar{\bar{\Gamma}}_{WB}}(\bar{R}, \bar{R}') = \bar{\bar{\Gamma}}_{WB}(\bar{R}', \bar{R}) \tag{2.17}$$

and interchanging the primed and unprimed coordinates, Eq. (2.16) can be written in the form of

$$\bar{E}(\bar{R}) = jk_0 Z_0 \int_{V_j} \bar{\bar{\Gamma}}_{WB}(\bar{R}, \bar{R}') \cdot \bar{J}_v(\bar{R}')\,\mathrm{dv}. \tag{2.18}$$

Eq. (2.18) shows the desired relationship between the electric field intensity and the dyadic Green's function.

2.2 Construction of the Dyadic Green's Function

To simplify the derivation of the dyadic Green's function, vector Green's function is defined as follows,

$$\bar{G}(\bar{R}, \bar{R}') = \bar{\bar{\Gamma}}_{WB}(\bar{R}, \bar{R}') \cdot \hat{u} \tag{2.19}$$

where $\hat{u}$ is a unit vector in an arbitrary direction. If we take the dot product of the Eqs. (2.6), (2.7) and (2.8) with $\hat{u}$, it is easily seen that vector Green's function satisfies the following equations

$$\nabla \times \nabla \times \bar{G}(\bar{R}, \bar{R}') - k_0^2 \bar{G}_{WB}(\bar{R}, \bar{R}') = -\hat{u}\delta(\bar{R} - \bar{R}'). \tag{2.20}$$

$$\hat{n} \times \bar{G}(\bar{R}, \bar{R}') \Big|_{\bar{R} \text{ on } S_W} = 0, \tag{2.21}$$

$$\hat{n} \times \hat{n} \times \bar{G}(\bar{R}, \bar{R}') \Big|_{\bar{R} \text{ on } S_B} = \kappa \hat{n} \times \nabla \times \bar{G}(\bar{R}, \bar{R}') \Big|_{\bar{R} \text{ on } S_B} \tag{2.22}$$

and also the edge condition and the radiation condition on Σ. $\bar{G}(\bar{R}, \bar{R}')$ may be considered as the field due to a vector point source $\hat{u}\delta(\bar{R}-\bar{R}')$ located at $\bar{R}'$. After determining $\bar{G}(\bar{R}, \bar{R}')$, dyadic Green's function can be found by using Eq. (2.19).

The solution of the inhomogeneous differential equation in Eq. (2.20) is obtained by superimposing the corresponding homogeneous differential equation,

$$\nabla \times \nabla \times \bar{F} - k_0^2 \bar{F} = 0. \tag{2.23}$$

Singularity introduced by the impulse function serves to divide the Volume V into two source free regions of I and II. Volume V is divided by the spherical surface S_D at $r = r'$ which contains the source point. At the dividing surface the Green's function is continuous but its derivatives are discontinuous in order to satisfy the singularity introduced by the impulse function.

It has been pointed out in [11] and [12] that the spherical vector wave functions which are defined in Appendix A, are set of orthogonal vector wave functions that are complete with respect to the class of functions which are solution of the vector wave equation given in Eq. (2.23). Consequently, $\bar{G}(\bar{R}, \bar{R}')$ can be expanded in terms of these solenoidal vector wave functions as

$$\bar{G}^I = \sum_q a_q(\bar{R}') \bar{M}^I_{\substack{e \\ o}\, q}(k_0 \bar{R}) + b_q(\bar{R}') \bar{N}^I_{\substack{e \\ o}\, q}(k_0 \bar{R}) \tag{2.24}$$

$$\bar{G}^{II} = \sum_q c_q(\bar{R}') \bar{M}^{II}_{\substack{e \\ o}\, q}(k_0 \bar{R}) + d_q(\bar{R}') \bar{N}^{II}_{\substack{e \\ o}\, q}(k_0 \bar{R}) \tag{2.25}$$

where $\bar{G}^I$ and $\bar{G}^{II}$ are the valid Green's functions in the region I and region II, respectively. q is the compact summation index. $\bar{M}^e_{\substack{e \\ o}\, q}$ and $\bar{N}^e_{\substack{e \\ o}\, q}$ are solenoidal vector wave functions which are defined in Eqs. (A.13) and (A.14).

Imposing the boundary condition at S_W, Eq. (2.21), results in the following expressions

$$\hat{\phi} \times \bar{M}^{I,II}_{\substack{e \\ o}\, q}(k_0 \bar{R}) \Big|_{\phi=0,\gamma} = 0 \tag{2.26}$$

$$\hat{\phi} \times \bar{N}^{I,II}_{\substack{e \\ o}\, q}(k_0 \bar{R}) \Big|_{\phi=0,\gamma} = 0 \tag{2.27}$$

Using the explicit expression for vector wave functions given in Eqs. (A.18)–(A.23) expressions reduce to

$$\frac{\mp\mu \begin{matrix}\sin\\ \cos\end{matrix}(\mu\phi)T^{-\mu}_{\mu+n}(\cos\theta)}{\sin\theta}\Big|_{\phi=0,\gamma} = 0 \tag{2.28}$$

$$\begin{matrix}\cos\\ \sin\end{matrix}(\mu\phi)\frac{d}{d\theta}[T^{-\mu}_{\mu+n}(\cos\theta)]\Big|_{\phi=0,\gamma} = 0 \tag{2.29}$$

where $T^{-\mu}_{\mu+n}(\cos\theta)$ is the Ferrer's type associated Legendre function. It can be seen that in order to satisfy the boundary condition at $\phi = 0$, $\sin(\mu\phi)$ functions should be chosen. As a result, $\bar{M}$ and $\bar{N}$ functions are chosen as even and odd, respectively. To satisfy the boundary condition at $\phi = \gamma$, eigenvalues for μ is defined as

$$\mu = \frac{m\pi}{\gamma} \qquad m = 0, 1, 2, \ldots \tag{2.30}$$

$\bar{G}^I$ should satisfy the impedance boundary condition (Eq. (2.22)) on S_B

$$\begin{aligned}&\hat{r}\times\hat{r}\times\sum_q[a_q(\bar{R}')\bar{M}^I_{eq}(k_0\bar{R}) + b_q(\bar{R}')\bar{N}^I_{oq}(k_0\bar{R})]\\ &= \kappa\hat{r}\times\nabla\times\sum_p[a_p(\bar{R}')\bar{M}^I_{ep}(k_0\bar{R}) + b_p(\bar{R}')\bar{N}^I_{op}(k_0\bar{R})]\end{aligned} \tag{2.31}$$

where q is compact summation index for μ, n and p is the compact summation index representing μ', n'. Using the symmetry relation of the vector wave functions given in Eqs. (A.16) and (A.17), right hand side of the Eq. (2.31) can be simplified, resulting as

$$\begin{aligned}&\hat{r}\times\hat{r}\times\sum_q[a_q(\bar{R}')\bar{M}^I_{eq}(k_0\bar{R}) + b_q(\bar{R}')\bar{N}^I_{oq}(k_0\bar{R})]\\ &= \kappa k_0\hat{r}\times\sum_p[a_p(\bar{R}')\bar{N}^I_{ep}(k_0\bar{R}) + b_p(\bar{R}')\bar{M}^I_{op}(k_0\bar{R})]\end{aligned} \tag{2.32}$$

Expressing the relations in terms of auxiliary vector wave functions using the Eqs. (A.18)–(A.23), and taking the cross products, expression reduces to

$$\begin{aligned}&-\sum_q\{a_q(\bar{R}')k_0 z^{(IM)}_{\mu+n}(k_0 r)\bar{m}_{e\mu n}(\theta,\phi) + b_q(\bar{R}')\frac{1}{r}\frac{d}{dr}[r z^{(IN)}_{\mu+n}(kr)]\bar{n}_{o\mu n}(\theta,\phi)\}\\ &= k_0\kappa\sum_p\{-a_p(\bar{R}')\frac{1}{r}\frac{d}{dr}[r z^{(IN)}_{\mu'+n'}(kr)]\bar{m}_{e\mu' n'}(\theta,\phi) + b_p(\bar{R}')k_0 z^{(IN)}_{\mu'+n'}(kr)\bar{n}_{o\mu' n'}(\theta,\phi)\}\end{aligned} \tag{2.33}$$

which should be evaluated at the surface of the spherical scatterer, $r = a$. In Eq. (2.33), $\bar{m}^{e}_{o\mu n}$ and $\bar{n}^{e}_{o\mu n}$ are the auxiliary vector wave functions defined in Eqs. (A.20) and (A.22). $z^{(IM)}_{\mu+n}(kr)$ and $z^{(IN)}_{\mu+n}(kr)$ are the combination of spherical Bessel and Hankel functions. Applying the orthogonality of the auxiliary vector wave function over the spherical surface given in Eq. (A.28), expression in Eq. (2.33) can be written as

$$\sum_{q}\{a_q(\bar{R}')\left[\frac{k_0\kappa}{r}\frac{d}{dr}[rz^{(IM)}_{\mu+n}(kr)] - k_0 z^{(IM)}_{\mu+n}(k_0 r)\right]\bar{m}_{e\mu n}(\theta,\phi)$$
$$-b_q(\bar{R}')\left[\frac{1}{r}\frac{d}{dr}[rz^{(IN)}_{\mu+n}(kr)] + k_0^2\kappa z^{(IM)}_{\mu+n}(k_0 r)\right]\bar{n}_{o\mu n}(\theta,\phi)\}\Big|_{r=a} = 0 \tag{2.34}$$

Consequently, following equations should be satisfied

$$\frac{k_0\kappa}{r}\frac{d}{dr}[rz^{(IM)}_{\mu+n}(kr)] - k_0 z^{(IM)}_{\mu+n}(k_0 r)\Big|_{r=a} = 0 \tag{2.35}$$

$$\frac{1}{r}\frac{d}{dr}[rz^{(IN)}_{\mu+n}(kr)] + k_0^2\kappa z^{(IM)}_{\mu+n}(k_0 r)\Big|_{r=a} = 0 \tag{2.36}$$

Solving Eqs. (2.35) and (2.36), radial functions are found as,

$$z^{(IM)}_{\mu+n}(k_0 r) = j_{\mu+n}(k_0 r) + \alpha_{\mu n}(k_0 a)h^{(2)}_{\mu+n}(k_0 r) \tag{2.37}$$

$$z^{(IN)}_{\mu+n}(k_0 r) = j_{\mu+n}(k_0 r) + \beta_{\mu n}(k_0 a)h^{(2)}_{\mu+n}(k_0 r) \tag{2.38}$$

where

$$\alpha_{\mu n}(k_0 a) = -\frac{k_0\kappa j'_{\mu+n}(k_0 a) + (\frac{\kappa}{a}-1)j_{\mu+n}(k_0 a)}{k_0\kappa h^{(2)\prime}_{\mu+n}(k_0 a) + (\frac{\kappa}{a}-1)h^{(2)}_{\mu+n}(k_0 a)} \tag{2.39}$$

$$\beta_{\mu n}(k_0 a) = -\frac{k_0 j'_{\mu+n}(k_0 a) + (\frac{1}{a}+k_0^2\kappa)j_{\mu+n}(k_0 a)}{k_0 h^{(2)\prime}_{\mu+n}(k_0 a) + (\frac{1}{a}+k_0^2\kappa)h^{(2)}_{\mu+n}(k_0 a)} \tag{2.40}$$

In Eqs. (2.39) and (2.40), $j_{\mu+n}(k_0 r)$ and $h^{(2)}_{\mu+n}(k_0 r)$ represent the spherical Bessel function and the spherical Hankel function of the second kind, respectively. Primes denote the derivatives of the functions with respect to their argument.

Since $G^{II}(\bar{R},\bar{R}')$ must satisfy the radiation condition on Σ, the appropriate radial function in this region is Hankel function of second kind which is denoted by superscript (4).

As discussed in Appendix A, edge condition is satisfied by choosing the order and index of the Ferrer type Legendre functions such that their sum is an integer [12].

Finally, vector Green's function in source free regions are

$$\bar{G}^I = \sum_q a_q(\bar{R}')\bar{M}_{eq}^{(IM)}(k_0\bar{R}) + b_q(\bar{R}')\bar{N}_{oq}^{(IN)}(k_0\bar{R}) \qquad \bar{R} \text{ in region } I \tag{2.41}$$

$$\bar{G}^{II} = \sum_q c_q(\bar{R}')\bar{M}_{eq}^{(4)}(k_0\bar{R}) + d_q(\bar{R}')\bar{N}_{oq}^{(4)}(k_0\bar{R}) \qquad \bar{R} \text{ in region } II. \tag{2.42}$$

To solve for the unknown coefficients a_q, b_q, c_q and d_q, Green's second identity is applied over the regions I and II.

In order to calculate c_q consider Green's second identity,

$$\begin{aligned} &\int_V (\bar{B} \cdot \nabla \times \nabla \times \bar{A} - \bar{A} \cdot \nabla \times \nabla \times \bar{B})\mathrm{dv} \\ &= \int_{S'} [(\hat{n} \times \bar{A}) \cdot (\nabla \times \bar{B}) - (\hat{n} \times \bar{B}) \cdot (\nabla \times \bar{A})]\mathrm{ds} \end{aligned} \tag{2.43}$$

and substitute

$$\bar{A} = \bar{G}(\bar{R}, \bar{R}') \tag{2.44}$$

$$\bar{B} = \bar{M}_{eq'}^{(IM)}(k_0\bar{R}) \tag{2.45}$$

Volume V_1 represents the region I shown in Fig. 2.1 and S' consists of surfaces S_W, S_B and S_D. Using Eqs. (2.20) and (2.23), left hand side of Eq. (2.43) becomes,

$$\begin{aligned} -\hat{u} \cdot \bar{M}_{eq'}^{(IM)}(k_0\bar{R}) = \int_{S'} &\{[\hat{n} \times \bar{G}(\bar{R}, \bar{R}')] \cdot [\nabla \times \bar{M}_{eq'}^{(IM)}(k_0\bar{R})] \\ - &[\hat{n} \times \bar{M}_{eq'}^{(IM)}(k_0\bar{R})] \cdot [\nabla \times \bar{G}(\bar{R}, \bar{R}')]\}\mathrm{ds} \end{aligned} \tag{2.46}$$

Both $\bar{M}_{eq'}^{(IM)}$ and $\bar{G}$, satisfy the boundary condition on the surface of the wedge, consequently, integration on S_W vanishes. In addition, they also satisfy the impedance boundary condition on S_B, therefore, using the similar procedure to Eq. (2.15), integration on S_B also vanishes. Hence, limits of the integration reduces to S_D. As discussed earlier, Green's function is continuous at $r = r'$, therefore we can write

$$\hat{n} \times \bar{G}(\bar{R}, \bar{R}') = \hat{r} \times \bar{G}^{II}(\bar{R}, \bar{R}') \tag{2.47}$$

$$\nabla \times \bar{G}(\bar{R}, \bar{R}') = \nabla \times \bar{G}^{II}(\bar{R}, \bar{R}') \tag{2.48}$$

Substituting these equations in Eq. (2.46) and using the pair relations given in Eqs. (A.16) and (A.17), integration on S_D reduces to

$$-\hat{u} \centerdot \bar{M}_{eq'}^{(IM)}(k_0\bar{R}) = k_0 \sum_q c_q(\bar{R}')C_q + d_q(\bar{R}')D_q \tag{2.49}$$

where

$$C_q = \int_{S_D} [\hat{r} \times \bar{M}_{eq}^{(4)}(k_0\bar{R}) \centerdot \bar{N}_{eq'}^{(IM)}(k_0\bar{R}) - \hat{r} \times \bar{M}_{eq'}^{(IM)}(k_0\bar{R}) \centerdot \bar{N}_{eq}^{(4)}(k_0\bar{R})]\mathrm{d}s \tag{2.50}$$

and

$$D_q = \int_{S_D} [\hat{r} \times \bar{N}_{oq}^{(4)}(k_0\bar{R}) \centerdot \bar{N}_{eq'}^{(IM)}(k_0\bar{R}) - \hat{r} \times \bar{M}_{eq'}^{(IM)}(k_0\bar{R}) \centerdot \bar{M}_{oq}^{(4)}(k_0\bar{R})]\mathrm{d}s. \tag{2.51}$$

If we express the integration in terms of the auxiliary vector wave functions, D_q becomes

$$\begin{aligned} D_q = \quad & - \quad \{\frac{\frac{d}{dr}[rz_{\mu+n}^{(4)}(k_0r)]\frac{d}{dr}[rz_{\mu'+n'}^{(IM)}(k_0r)]}{r^2}\} + k_0^2 z_{\mu'+n'}^{(IM)}(k_0r) z_{\mu+n}^{(4)}(k_0r)\} \Big|_{r=r'} \\ & \cdot \quad \int_0^\gamma \int_0^\pi \bar{m}_{oq}(\theta,\phi) \centerdot \bar{n}_{eq'}(\theta,\phi)\,\mathrm{d}\theta\mathrm{d}\phi \end{aligned} \tag{2.52}$$

According to the orthogonality of the auxiliary vector wave functions we conclude that,

$$D_q = 0. \tag{2.53}$$

Expressing C_q in terms of auxiliary functions, Eq. (2.50) becomes

$$\begin{aligned} C_q \quad = \quad & k_0 \frac{1}{r}\{z_{\mu+n}^{(4)}(k_0r)\frac{d}{dr}[rz_{\mu'+n'}^{(IM)}(k_0r)] - \frac{d}{dr}[rz_{\mu+n}^{(4)}(k_0r)] z_{\mu'+n'}^{(IM)}(k_0r)\} \Big|_{r=r'} \\ & \cdot \quad r'^2 \int_0^\gamma \int_0^\pi \bar{n}_{eq}(\theta,\phi) \centerdot \bar{n}_{eq'}(\theta,\phi)\,\mathrm{d}\theta\mathrm{d}\phi \end{aligned} \tag{2.54}$$

Using the Wronskian relation of the spherical Bessel and Hankel function [13],

$$W[j_n(x), h_n^{(2)}(x)] = \frac{1}{jx^2} \tag{2.55}$$

and the orthogonality relations, C_q is found as,

$$C_q = j\frac{\epsilon_m \gamma n!(\mu+n)(\mu+n+1)}{(2\mu+2n+1)\Gamma(2\mu+n+1)} \tag{2.56}$$

Finally using Eqs. (2.49), (2.54) and (2.53), we have

$$c_q(R') = \frac{\pi j}{2k_0} \frac{1}{Q_{\mu n}(\mu+n)(\mu+n+1)} \bar{M}_{eq}^{(IM)}(k_0\bar{R}') \cdot \hat{u} \tag{2.57}$$

where

$$Q_{\mu n} = \frac{\epsilon_m \pi \gamma n!}{2(2\mu+2n+1)\Gamma(2\mu+n+1)}. \tag{2.58}$$

Following the same procedure but this time substituting

$$\bar{B} = \bar{N}_{oq'}^{(IN)}(k_0\bar{R}), \tag{2.59}$$

d_q can be found as

$$d_q(\bar{R}') = \frac{\pi j}{2k_0} \frac{1}{Q_{\mu n}(\mu+n)(\mu+n+1)} \bar{M}_{eq}^{(IN)}(k_0\bar{R}') \cdot \hat{u}. \tag{2.60}$$

To solve for a_q and b_q, the same procedure is repeated but this time integrating over region II. To obtain a_q, choose

$$\bar{A} = \bar{G}(\bar{R}, \bar{R}') \tag{2.61}$$

$$\bar{B} = \bar{M}_{eq'}^{(4)}(k_0\bar{R}) \tag{2.62}$$

and after applying the Green's second, Eq. (2.43) reduces to,

$$\begin{aligned} -\hat{u} \cdot \bar{M}_{eq'}^{(4)}(k_0\bar{R}) = & \int_S \{[\hat{n} \times \bar{G}(\bar{R}, \bar{R}')] \cdot [\nabla \times \bar{M}_{eq'}^{(4)}(k_0\bar{R})] \\ & - [\hat{n} \times \bar{M}_{eq'}^{(4)}(k_0\bar{R})] \cdot [\nabla \times \bar{G}(\bar{R}, \bar{R}')]\} \mathrm{ds} \end{aligned} \tag{2.63}$$

where surface S consists of S_W, S_D and Σ. Because of the boundary condition on surface of the wedge, integration on S_W vanishes. Furthermore, $\bar{G}(\bar{R}, \bar{R}')$ and $\bar{M}_{eq'}^{(4)}$ satisfy the radiation condition on Σ. Hence, integration on this surface also vanishes. Across the Dividing surface S_D, Green's function can be assumed continuous so that,

$$\hat{n} \times \bar{G}(\bar{R}, \bar{R}') = -\hat{r} \times \bar{G}^I(\bar{R}, \bar{R}') \tag{2.64}$$

$$\nabla \times \bar{G}(\bar{R}, \bar{R}') = \nabla \times \bar{G}^I(\bar{R}, \bar{R}') \tag{2.65}$$

Eq. (2.63) can be further simplified as

$$-\hat{u} \cdot \bar{M}_{eq'}^{(4)}(k_0\bar{R}) = k_0 \sum_q a_q(\bar{R}') A_q + b_q(\bar{R}') B_q \tag{2.66}$$

where

$$A_q = \int_{S_D} [-\hat{r} \times \bar{M}_{eq}^{(IM)}(k_0\bar{R}) \centerdot \bar{N}_{eq'}^{(4)}(k_0\bar{R}) + \hat{r} \times \bar{M}_{eq'}^{(4)}(k_0\bar{R}) \centerdot \bar{N}_{eq}^{(IM)}(k_0\bar{R})]\mathrm{d}s \quad (2.67)$$

and

$$B_q = \int_{S_D} [-\hat{r} \times \bar{N}_{oq}^{(IN)}(k_0\bar{R}) \centerdot \bar{N}_{eq'}^{(4)}(k_0\bar{R}) + \hat{r} \times \bar{M}_{eq'}^{(4)}(k_0\bar{R}) \centerdot \bar{M}_{oq}^{(IN)}(k_0\bar{R})]\mathrm{d}s. \quad (2.68)$$

Expressing the equations in terms of the auxiliary vector wave functions,

$$\begin{aligned} A_q &= k_0 \frac{1}{r} \{-z_{\mu+n}^{(IM)}(k_0 r) \frac{d}{dr}[r z_{\mu'+n'}^{(4)}(k_0 r)] + \frac{d}{dr}[r z_{\mu+n}^{(IM)}(k_0 r)] z_{\mu'+n'}^{(4)}(k_0 r)\} \Big|_{r=r'} \\ &\cdot \quad r'^2 \int_0^{\gamma} \int_0^{\pi} \bar{n}_{eq}(\theta,\phi) \centerdot \bar{n}_{eq'}(\theta,\phi)\, \mathrm{d}\theta \mathrm{d}\phi \end{aligned} \quad (2.69)$$

$$\begin{aligned} B_q &= \{\frac{\frac{d}{dr}[r z_{\mu+n}^{(IN)}(k_0 r)] \frac{d}{dr}[r z_{\mu'+n'}^{(4)}(k_0 r)]}{r^2}\} + k_0^2 z_{\mu'+n'}^{(4)}(k_0 r) z_{\mu+n}^{(IN)}(k_0 r)\} \Big|_{r=r'} \\ &\cdot \quad \int_0^{\gamma} \int_0^{\pi} \bar{m}_{oq}(\theta,\phi) \centerdot \bar{n}_{eq'}(\theta,\phi)\, \mathrm{d}\theta \mathrm{d}\phi \end{aligned} \quad (2.70)$$

Due to the orthogonality of the auxiliary vector wave functions (see Appendix A),

$$B_q = 0 \quad (2.71)$$

and

$$A_q = j \frac{\epsilon_m \gamma n! (\mu+n)(\mu+n+1)}{(2\mu+2n+1)\Gamma(2\mu+n+1)} \quad (2.72)$$

using Eqs. (2.72), (2.71) and (2.66), a_q is found to be

$$a_q(R') = \frac{\pi j}{2k_0} \frac{1}{Q_{\mu n}(\mu+n)(\mu+n+1)} \bar{M}_{eq}^{(4)}(k_0\bar{R}') \centerdot \hat{u}. \quad (2.73)$$

Following the same steps but this time with

$$\bar{B} = \bar{M}_{oq'}^{(4)}(k_0\bar{R}), \quad (2.74)$$

one could obtain

$$b_q(R') = \frac{\pi j}{2k_0} \frac{1}{Q_{\mu n}(\mu+n)(\mu+n+1)} \bar{N}_{oq}^{(4)}(k_0\bar{R}') \centerdot \hat{u}. \quad (2.75)$$

Substituting the unknown coefficients defined in Eqs. (2.57), (2.60) (2.73) and (2.75) in Eqs. (2.41)and (2.42), resulting Green's function is

$$\bar{G}^{I}(\bar{R},\bar{R}') = \frac{j\pi}{2k_0}\sum_{q}\Big[\frac{\bar{M}_{eq}^{(IM)}(k_0\bar{R})\bar{M}_{eq}^{(4)}(k_0\bar{R}') + \bar{N}_{oq}^{(IN)}(k_0\bar{R})\bar{N}_{oq}^{(4)}(k_0\bar{R}')}{Q_{\mu n}(\mu+n)(\mu+n+1)}\Big] \quad (2.76)$$

$$\bar{G}^{II}(\bar{R},\bar{R}') = \frac{j\pi}{2k_0}\sum_{q}\Big[\frac{\bar{M}_{eq}^{(4)}(k_0\bar{R})\bar{M}_{eq}^{(IM)}(k_0\bar{R}') + \bar{N}_{oq}^{(4)}(k_0\bar{R})\bar{N}_{oq}^{(IN)}(k_0\bar{R}')}{Q_{\mu n}(\mu+n)(\mu+n+1)}\Big] \quad (2.77)$$

Now, by comparing Eqs. (2.76) and (2.77) with Eq. (2.19) and adding the source correction term [8], complete dyadic Green's function for the impedance boss and the wedge is

$$\begin{aligned}\bar{\bar{\Gamma}}_{WB}(\bar{R},\bar{R}') &= \frac{\hat{r}\hat{r}}{k_0^2}\,\delta(\bar{R}-\bar{R}') \\ &+ \frac{j\pi}{2k_0}\begin{cases}\sum_{m=0}^{\infty}\sum_{n=0}^{\infty}\frac{\bar{M}_{e\mu n}^{(4)}(k_0\bar{R})\bar{M}_{e\mu n}^{(IM)}(k_0\bar{R}')+\bar{N}_{o\mu n}^{(4)}(k_0\bar{R})\bar{N}_{o\mu n}^{(IN)}(k_0\bar{R}')}{Q_{\mu n}(\mu+n)(\mu+n+1)} & r \geqslant r' \\ \sum_{m=0}^{\infty}\sum_{n=0}^{\infty}\frac{\bar{M}_{e\mu n}^{(IM)}(k_0\bar{R})\bar{M}_{e\mu n}^{(4)}(k_0\bar{R}')+\bar{N}_{o\mu n}^{(IN)}(k_0\bar{R})\bar{N}_{o\mu n}^{(4)}(k_0\bar{R}')}{Q_{\mu n}(\mu+n)(\mu+n+1)} & r \leqslant r'.\end{cases}\end{aligned} \quad (2.78)$$

To isolate the effects of the impedance scatterer and its interaction with the wedge, dyadic Green's function can be decomposed as

$$\bar{\bar{\Gamma}}_{WB}(\bar{R},\bar{R}') = \bar{\bar{\Gamma}}_{B}(\bar{R},\bar{R}') + \bar{\bar{\Gamma}}_{W}(\bar{R},\bar{R}') \quad (2.79)$$

Considering Eqs. (2.37) and (2.38), $\bar{M}_{e\mu n}^{(IM)}$ and $\bar{N}_{o\mu n}^{(IN)}$ can be written as

$$\bar{M}_{e\mu n}^{(IM)}(k_0\bar{R}) = \bar{M}_{e\mu n}^{(1)}(k_0\bar{R}) + \alpha_{\mu n}(k_0 a)\bar{M}_{e\mu n}^{(4)}(k_0\bar{R}) \quad (2.80)$$

$$\bar{N}_{o\mu n}^{(IN)}(k_0\bar{R}) = \bar{N}_{o\mu n}^{(1)}(k_0\bar{R}) + \beta_{\mu n}(k_0 a)\bar{N}_{o\mu n}^{(4)}(k_0\bar{R}) \quad (2.81)$$

Substituting these equations in Eq. (2.78), components of the dyadic Green's function are defined as follows,

$$\begin{aligned}\bar{\bar{\Gamma}}_W(\bar{R},\bar{R}') &= \frac{\hat{r}\hat{r}}{k_0^2}\,\delta(\bar{R}-\bar{R}') \\ &+ \frac{j\pi}{2k_0}\begin{cases}\sum_{m=0}^{\infty}\sum_{n=0}^{\infty}\frac{\bar{M}^{(4)}_{e\mu n}(k_0\bar{R})\bar{M}^{(1)}_{e\mu n}(k_0\bar{R}')+\bar{N}^{(4)}_{o\mu n}(k_0\bar{R})\bar{N}^{(1)}_{o\mu n}(k_0\bar{R}')}{Q_{\mu n}(\mu+n)(\mu+n+1)} & r \geqslant r' \\ \sum_{m=0}^{\infty}\sum_{n=0}^{\infty}\frac{\bar{M}^{(1)}_{e\mu n}(k_0\bar{R})\bar{M}^{(4)}_{e\mu n}(k_0\bar{R}')+\bar{N}^{(1)}_{o\mu n}(k_0\bar{R})\bar{N}^{(4)}_{o\mu n}(k_0\bar{R}')}{Q_{\mu n}(\mu+n)(\mu+n+1)} & r \leqslant r'.\end{cases}\end{aligned} \tag{2.82}$$

$$\begin{aligned}\bar{\bar{\Gamma}}_B(\bar{R},\bar{R}') = \sum_{m=0}^{\infty}\sum_{n=0}^{\infty} \quad &\{\tfrac{\alpha_{\mu n}(k_0a)}{Q_{\mu n}(\mu+n)(\mu+n+1)}\bar{M}^{(4)}_{e\mu n}(k_0\bar{R}')\bar{M}^{(4)}_{e\mu n}(k_0\bar{R}) \\ &+\tfrac{\beta_{\mu n}(k_0a)}{Q_{\mu n}(\mu+n)(\mu+n+1)}\bar{N}^{(4)}_{o\mu n}(k_0\bar{R}')\bar{N}^{(4)}_{o\mu n}(k_0\bar{R})\}\end{aligned} \tag{2.83}$$

where $\bar{\bar{\Gamma}}_W$ is the dyadic Green's function of the wedge with scatterer removed which is defined in [12]. $\bar{\bar{\Gamma}}_B$ is defined as the dyadic Green's function of the impedance boss. It includes the terms added due to the presence of the spherical scatterer which represents the scattering from the sphere and its interaction with the wedge. It should be noted that $\bar{\bar{\Gamma}}_B$ lacks the source correction term because it is accounted for $\bar{\bar{\Gamma}}_W$.

For the limiting case of a PEC scatterer, $\eta = 0$,

$$\alpha_{\mu n}(k_0a)\Big|_{\kappa=0} = -\frac{j_{\mu+n}(k_0a)}{h^{(2)}_{\mu+n}(k_0a)} \tag{2.84}$$

$$\beta_{\mu n}(k_0a)\Big|_{\kappa=0} = -\frac{j_{\mu+n}(k_0a)+k_0aj'_{\mu+n}(k_0a)}{h^{(2)}_{\mu+n}(k_0a)+k_0ah^{(2)'}_{\mu+n}(k_0a)} \tag{2.85}$$

and $\bar{\bar{\Gamma}}_B$ reduces to the dyadic Green's function of PEC boss derived in [12].

2.3 Comments on the Dyadic Green's function

In order to calculate the electric field, Eq. (2.78) is substituted into Eq. (2.18) which is as follows,

$$\bar{E}(\bar{R}) = jk_0 Z_0 \int_{V_j} \bar{\bar{\Gamma}}_{WB}(\bar{R}, \bar{R}') \cdot \bar{J}_v(\bar{R}') \, \mathrm{dv},$$

however, order of summation and integration should be changed and summation operations should be preceded by term by term integration to find the electric field [12].

Dyadic Green's function given in Eq. (2.78) is discontinuous at $\bar{R} = \bar{R}'$ due to the delta function. Besides, remaining series also diverges at $r = r'$. It is pointed out in [14] that eigenfunction expansion of the Green's function has discontinuous behavior over the spherical surface which contains the point source and these singularities can be modeled by a surface current at $r = r'$. Hence, vicinity of the source region should be avoided where the series does not converge. However, for physical current distributions, the series converges to a continuous function everywhere in space.

$\theta_0 = 80°$, $a = \lambda/4$		$\theta_0 = 80°$, $WA = 0°$		$WA = 0°$, $a = \lambda/4$	
WA	# of terms	a/λ	# of terms	θ_0	# of terms
0°	91	0.05	28	1°	36
30°	84	0.1	45	10°	50
60°	77	0.25	91	20°	63
90°	70	0.5	171	40°	77
120°	63	1	392	60°	72
150°	56	1.5	666	80°	91
180°	43				
210°	35				
240°	28				
270°	21				
300°	15				
330°	8				

Table 2.1: Number of terms retained in the eigenfunction solution for 6 digit accuracy

Convergence of the series is tested based on numerical results. For the far-field calculation of the scattered field, truncations size depends on the radius of the boss, wedge angle and also the position of the source. In Table 2.1, number of terms retained in the series given in Eqs. (2.90) and (2.91) for calculating the backscattered field is tabulated. As the size of the boss and the exterior wedge angle increase, the number of terms retained in the series also increases. In addition, for elevation angles close to zero (the paraxial region) convergence is faster.

2.4 Numerical Results

To observe the effects of the spherical scatterer and its interaction with the wedge, scattered field is defined according to the $\bar{\bar{\Gamma}}_B$ as,

$$\bar{E}^s(\bar{R}) = jk_0 Z_0 \int_{V_j} \bar{\bar{\Gamma}}_B(\bar{R}, \bar{R}') \cdot \bar{J}_v(\bar{R}') dv'. \tag{2.86}$$

and a point source is assumed at $\bar{R}_0 = r_0 \hat{r}_0$

$$\bar{J}_v(\bar{R}') = \delta(\bar{R}' - \bar{R}_0)\bar{p}_e \tag{2.87}$$

where $\bar{p}_e$ is an electric dipole moment which is determined by the angular unit vectors $\hat{\theta}$ and $\hat{\phi}$. Choosing a point source has a computational advantage so that electrical field due to this source leads to the very summation in Eq. (2.78). Since point source is chosen, as stated earlier, in order to obtain convergent results, vicinity of $r = r_0$ should be avoided. Away from this region, valid results are achieved.

Mono-static scattering pattern of the spherical boss is obtained by placing the source and observation point at the far-field of the scatterer and asymptotic expression for the radial dependence of the vector wave functions are used. Asymptotic approximation for spherical Hankel functions are given in [13] using the proper identities we have

$$\lim_{r\to\infty} h^{(2)}_{\mu+n}(k_0 r) = \frac{1}{k_0 r}\, e^{j\frac{\pi}{2}(\mu+n+1)}\, e^{-jk_0 r} \tag{2.88}$$

$$\lim_{r\to\infty}\frac{1}{r}\frac{d}{dr}[rh^{(2)}_{\mu+n}(k_0r)] = \frac{1}{r}\,e^{j\frac{\pi}{2}(\mu+n)}\,e^{-jk_0r}. \tag{2.89}$$

Scattered field is calculated with elevation angle fixed at a value θ_0, and ϕ is varied from 0 to γ. $E^s_{\theta\theta}$ is defined as the scattered electric field in $\hat{\theta}$ direction when the incident field is in $\hat{\theta}$ direction ($\bar{p}_e = \hat{\theta}$) and $E^s_{\phi\phi}$ is defined as the scattered electric field in $\hat{\phi}$ direction when incident field is in $\hat{\phi}$ direction($\bar{p}_e = \hat{\phi}$).

$$\begin{aligned} E^s_{\theta\theta}(\bar{R}) &= \frac{j\pi}{2k_0}\sum_{m=0}^{\infty}\sum_{n=0}^{\infty}\frac{e^{2j\frac{\pi}{2}(\mu+n)}}{Q_{\mu n}(\mu+n)(\mu+n+1)} \\ &\cdot \{-\alpha_{\mu n}(k_0a)[\bar{m}_{e\mu n}(\theta_0,\phi)\centerdot\hat{\theta}]^2 + \beta_{\mu n}(k_0a)[\bar{n}_{o\mu n}(\theta_0,\phi)\centerdot\hat{\theta}]^2\} \\ &\cdot \frac{e^{-jk_0r'}}{r'}\,\frac{e^{-jk_0r}}{r} \end{aligned} \tag{2.90}$$

$$\begin{aligned} E^s_{\phi\phi}(\bar{R}) &= \frac{j\pi}{2k_0}\sum_{m=0}^{\infty}\sum_{n=0}^{\infty}\frac{e^{2j\frac{\pi}{2}(\mu+n)}}{Q_{\mu n}(\mu+n)(\mu+n+1)} \\ &\cdot \{-\alpha_{\mu n}(k_0a)[\bar{m}_{e\mu n}(\theta_0,\phi)\centerdot\hat{\phi}]^2 + \beta_{\mu n}(k_0a)[\bar{n}_{o\mu n}(\theta_0,\phi)\centerdot\hat{\phi}]^2\} \\ &\cdot \frac{e^{-jk_0r'}}{r'}\,\frac{e^{-jk_0r}}{r} \end{aligned} \tag{2.91}$$

In Figs. 2.2 – 2.8, mono-static scattering patterns are plotted for a spherical boss of radius $a = 0.25\lambda$ at the edge of a half-plane ($\gamma = 2\pi$) where the elevation angle is varied as $\theta_0 = 1^\circ, 5^\circ, 10^\circ, 20^\circ, 40^\circ, 60^\circ$, and 80°. Backscattered field is plotted for three different normalized surface impedance values, $\eta_s = \eta/Z_0 = 0, 1.5$ and 2, where $\eta_s = 0$ represents the PEC case.

It is observed that scattered field intensity is highly influenced by the incident and scattered field angles. For elevation angles close to zero, the paraxial region, scattered field is enhanced due to the powerful edge guided waves. As we move away from this region, edge effect diminishes and amplitude of the scattered field decreases.

Impedance of the boss also affects the scattering pattern. For low elevation angles, as the impedance of the scatterer increases, field intensity increases. However, for $\theta_0 = 60^\circ, 80^\circ$ shown in Figs. 2.7 and 2.8, impedance value does not affect the maximum field intensity significantly.

In the paraxial region, field pattern varies as $\cos^2(\frac{\phi}{2})$ and $\sin^2(\frac{\phi}{2})$ for $E^s_{\theta\theta}$ and $E^s_{\phi\phi}$, respectively which indicates that $n = 0, m = 1$ mode is dominant. As elevation angle θ_0 increases higher order modes are excited.

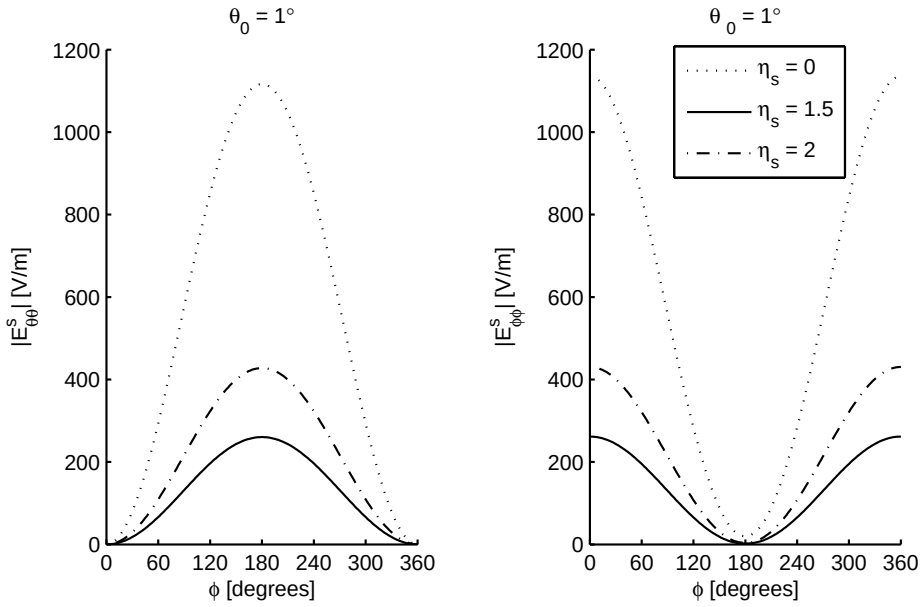

Figure 2.2: Monostatic scattered field pattern for $a = 0.25\lambda$, $\gamma = 2\pi$ and $\theta_0 = 1°$.

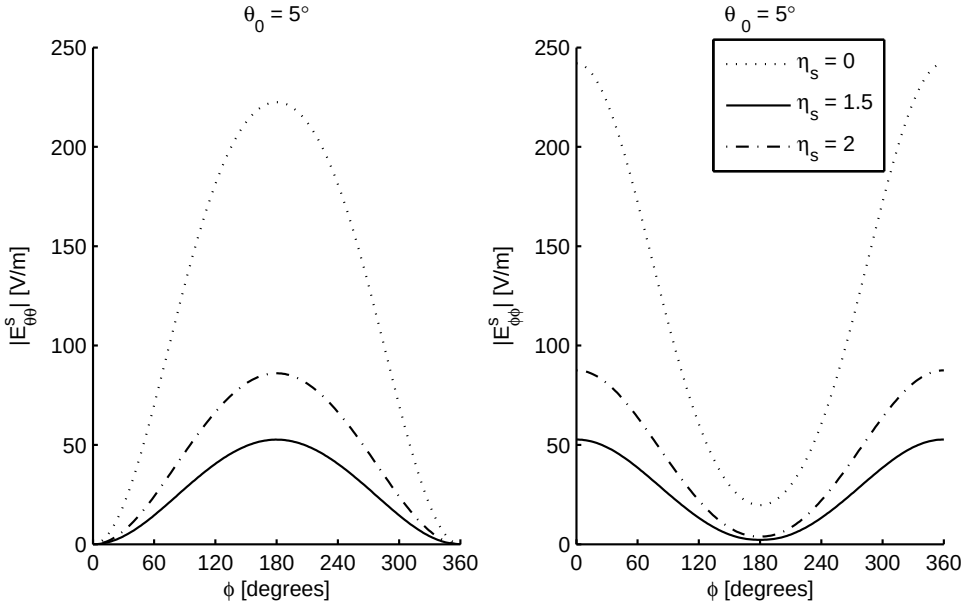

Figure 2.3: Monostatic scattered field pattern for $a = 0.25\lambda$, $\gamma = 2\pi$ and $\theta_0 = 5°$.

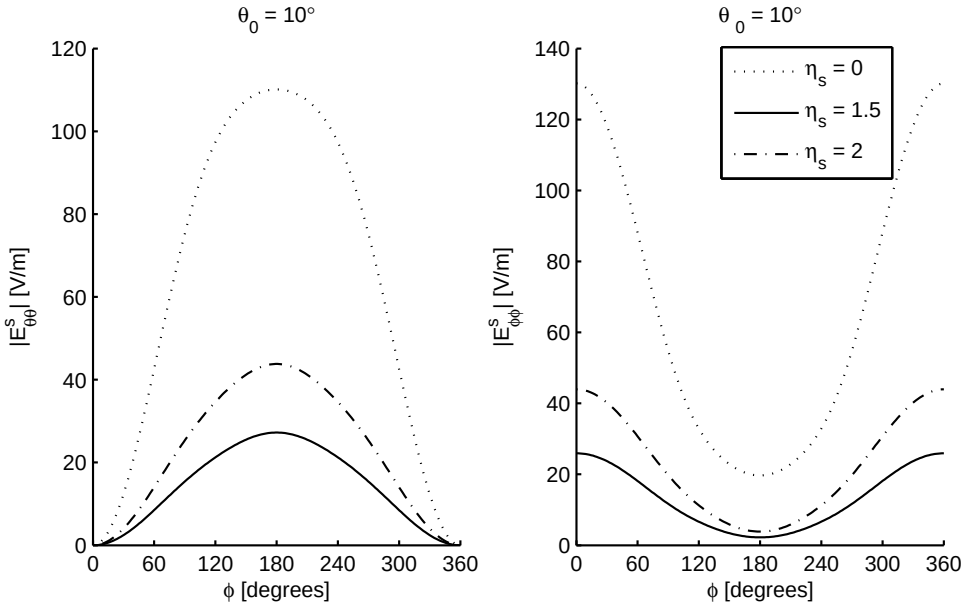

Figure 2.4: Monostatic scattered field pattern for $a = 0.25\lambda$, $\gamma = 2\pi$ and $\theta_0 = 10°$.

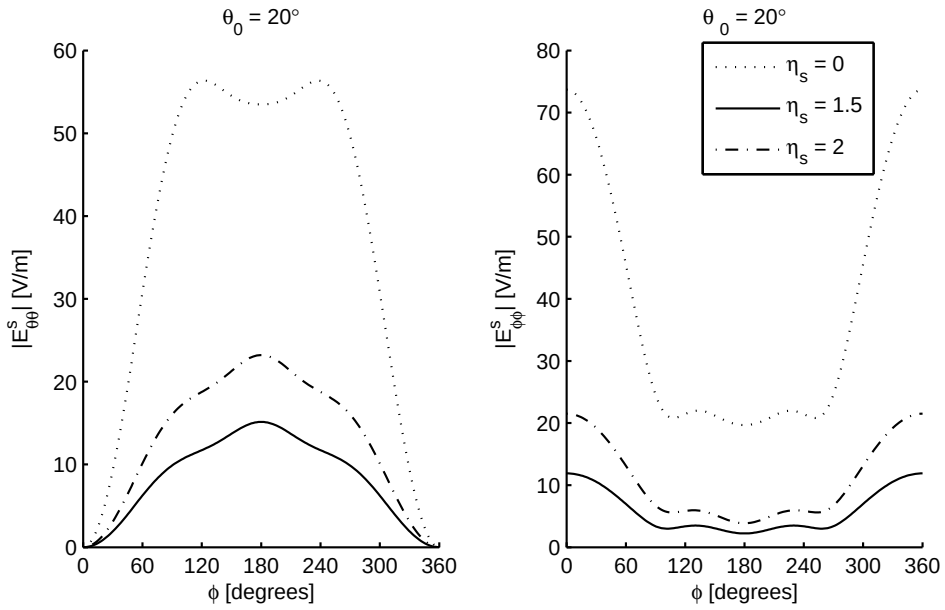

Figure 2.5: Monostatic scattered field pattern for $a = 0.25\lambda$, $\gamma = 2\pi$ and $\theta_0 = 20°$.

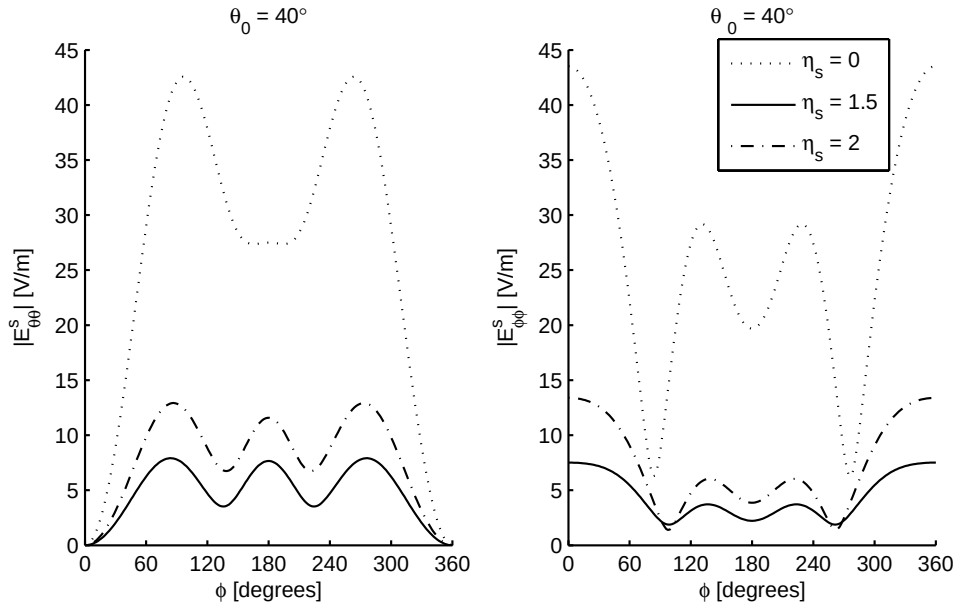

Figure 2.6: Monostatic scattered field pattern for $a = 0.25\lambda$, $\gamma = 2\pi$ and $\theta_0 = 40°$.

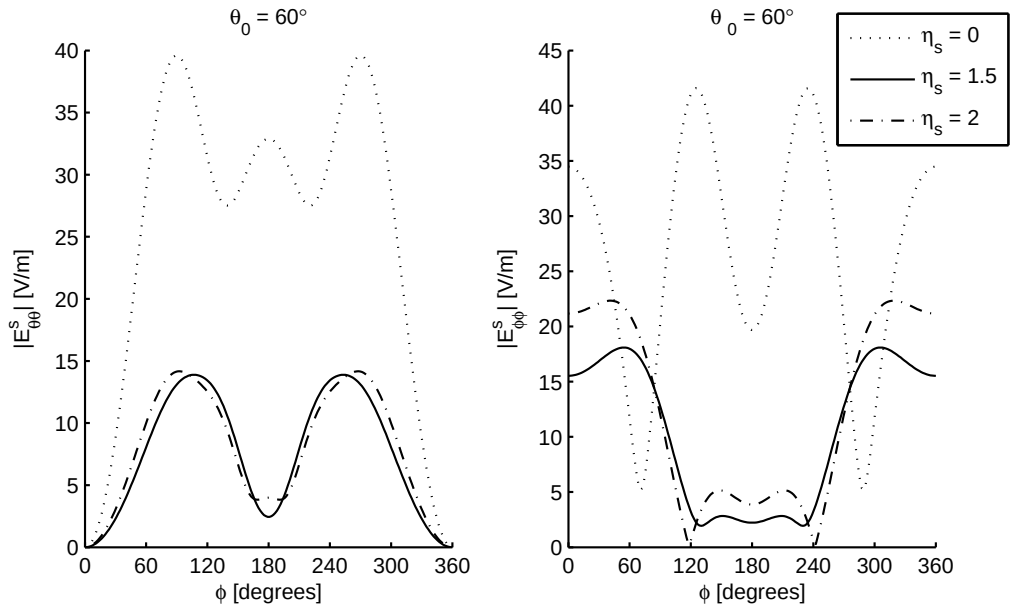

Figure 2.7: Monostatic scattered field pattern for $a = 0.25\lambda$, $\gamma = 2\pi$ and $\theta_0 = 60°$.

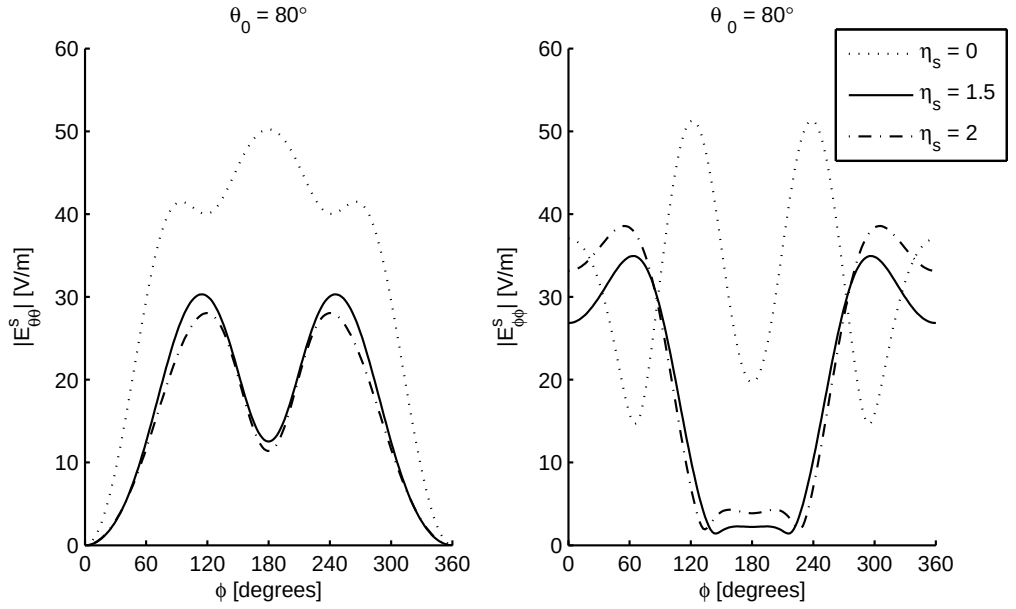

Figure 2.8: Monostatic scattered field pattern for $a = 0.25\lambda$, $\gamma = 2\pi$ and $\theta_0 = 80°$.

Chapter 3

T-Matrix Solution for Irregularly-Shaped impedance Scatterers at the Edge

In Chapter 2, the solution for a spherical impedance scatterer at the edge is presented. Here, general case of an irregularly shaped impedance scatterer is considered. T-matrix is a well suited numerical method to calculate the scattered field from non-spherical and non-circular objects which is introduced in [15, 16]. This method is primarily formulated based on the Huygen's principle in conjunction with extended boundary condition which states that induced currents on the obstacle cancel the incident field through out the interior volume of the scatterer.

Starting point for T-matrix method is applying the Green's second identity alongside with the appropriate Green's function over a portion of space and assume a null field inside of the volume. In the classical formulation, incident field is expanded using free-space Green's function but for our problem dyadic Green's function of the wedge will be used. Therefore incident field is defined as the field in the presence of the wedge with scatterer removed. Scattered field and the incident field will be expanded in terms of proper vector wave functions then

their coefficients will be related through using T-matrix. The analysis is an extension of the procedure outlined in [7] in which scattering from PEC objects are considered.

3.1 T-Matrix Formulation for Impedance Scatterer at the Edge

The Geometry of the problem is shown in Fig. 3.1. An infinitely long wedge is considered along the z-axis and scatterer is located at the edge. Center of the coordinates is defined inside the scatterer and $\bar{R}$ and $\bar{R}'$ points the observation and source locations. Incident field is defined as follows,

$$\bar{E}^i(\bar{R}) = jk_0 Z_0 \int_{V_j} \bar{\bar{\Gamma}}_W(\bar{R}, \bar{R}') \cdot \bar{J}_v(\bar{R}') \, \mathrm{dv}. \tag{3.1}$$

where $\bar{\bar{\Gamma}}_W$ is the dyadic Green's function of the wedge given in Eq. (2.82) and $\bar{J}_v(\bar{R}')$ is the volumetric current distribution confined to V_j. The total field can be represented as

$$\bar{E} = \bar{E}^i + \bar{E}^s \tag{3.2}$$

where $\bar{E}^s$ is the scattered field due to presence of the impedance scatterer which is same as the definition given in Chapter 2. Cross section of the geometry on the x-y plane is given in Fig. 3.1 where the origin is defined inside the scatterer. Surface of the scatterer is denoted as S_s and two imaginary surfaces of inscribing and circumscribing segment spheres are depicted which are denoted as S_i and S_c, respectively.

Applying the Green's second identity for $\bar{\bar{\Gamma}}_W$ and $\bar{E}(\bar{R})$, one could obtain,

$$\left.\begin{array}{cccc} \bar{R} & \text{outside} & S_s & \bar{E}(\bar{R}) \\ \bar{R} & \text{inside} & S_s & 0 \end{array}\right\} = \bar{E}^i(\bar{R}) + \int_S \Big\{ [\hat{n}' \times \bar{\bar{\Gamma}}_W(\bar{R}, \bar{R}')] \cdot [\nabla' \times \bar{E}(\bar{R}')] - [\hat{n}' \times \bar{E}(\bar{R}')] \cdot [\nabla' \times \bar{\bar{\Gamma}}_W(\bar{R}, \bar{R}')] \Big\} \, \mathrm{d}s' \tag{3.3}$$

where S consists of S_S, S_W, and Σ. It can be seen that, in the exterior region, Eq. (3.3) gives the scattered field in terms of the surface fields and in the interior

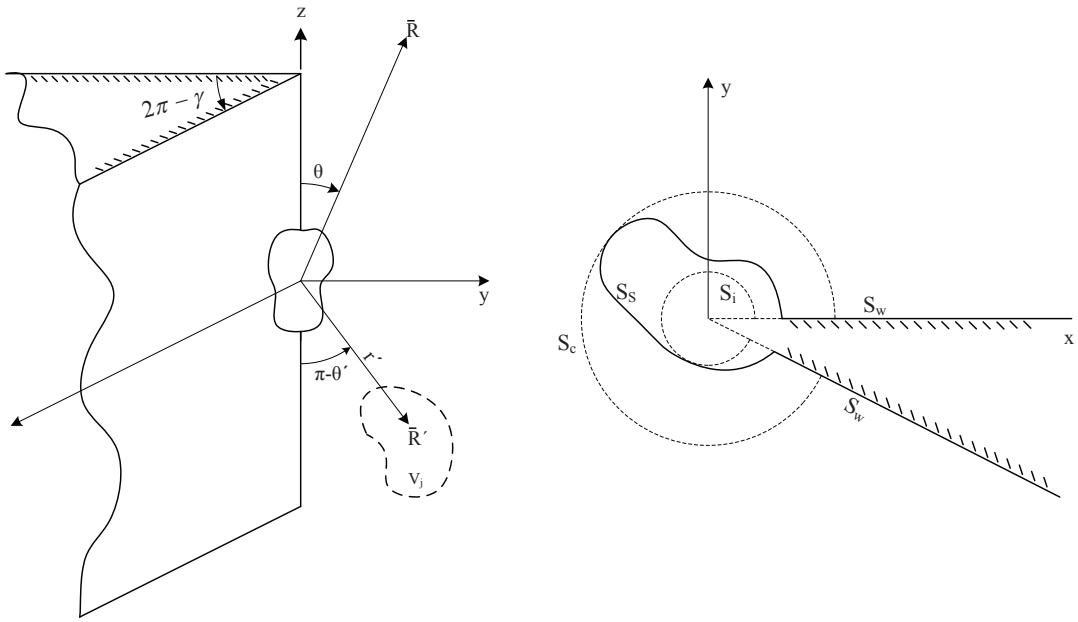

Figure 3.1: Geometry of an irregularly shaped object placed at the edge of a wedge

region fields expressed by the surface integrals are canceled out by the incident field. Due to the boundary condition on the surface of the wedge, integration on S_W will vanish. Integration on Σ will also result in zero because of the plane wave behavior of the fields in the far-field. Hence the integration will be evaluated just on the surface of the scatterer.

Spherical vector wave functions are complete set of functions which can be used to expand the electric field inside and outside of the scatterer. For the field points inside the inscribed sphere S_i, incident field can be written as

$$\bar{E}^i(\bar{R}) = \sum_q R_q[a_q \bar{M}_{eq}^{(1)}(k_0\bar{R}) + b_q \bar{N}_{oq}^{(1)}(k_0\bar{R})] \tag{3.4}$$

where

$$R_q = \frac{j\pi}{2k_0(\mu+n)(\mu+n+1)Q_{\mu n}}. \tag{3.5}$$

and q is the compact index representing $\mu\, n$. Since the field should be regular at the origin spherical Bessel functions denoted by superscript (1) are used. Scattered field outside the circumscribing sphere, S_c, is defined as

$$\bar{E}^s(\bar{R}) = \sum_p R_p[e_p \bar{M}_{ep}^{(4)}(k_0\bar{R}) + f_p \bar{N}_{op}^{(4)}] \tag{3.6}$$

Hankel functions, denoted by superscript (4), are chosen to satisfy the radiation condition.

Now, consider that $\bar{R}$ is on S_i which is a segment sphere centered at the origin totally inside the scatterer, and $\bar{R}'$ on S_s. In this case, considering that $r < r'$ dyadic Green's function of the wedge can be written as

$$\bar{\bar{\Gamma}}_W(\bar{R},\bar{R}') = \sum_q R_q[\bar{M}^{(1)}_{eq}(k_0\bar{R})\bar{M}^{(4)}_{eq}(k_0\bar{R}') + \bar{N}^{(1)}_{oq}(k_0\bar{R})\bar{N}^{(4)}_{oq}(k_0\bar{R}')] \tag{3.7}$$

Using the vector identity given in Eq. (2.11), and considering that $\bar{R}$ is inside S_S, Eq. (3.3) can be written as

$$-\bar{E}^i(\bar{R}) = \int_{S_s}\{-\bar{\bar{\Gamma}}_W(\bar{R},\bar{R}')\centerdot[\hat{n}'\times\nabla'\times\bar{E}(\bar{R}')] - [\hat{n}'\times\bar{E}(\bar{R}')]\centerdot[\nabla'\times\bar{\bar{\Gamma}}_W(\bar{R},\bar{R}')]\}\mathrm{d}s' \tag{3.8}$$

Electric field must satisfy the impedance boundary condition on S_S,

$$\hat{n}\times\hat{n}\times\bar{E}(\bar{R}) = \frac{\eta}{jk_0Z_0}\hat{n}\times\nabla\times\bar{E}(\bar{R}) \tag{3.9}$$

where η is the surface impedance of the scatterer. Applying the boundary condition, Eq. (3.8) reduces to,

$$-\bar{E}^i(\bar{R}) = \int_{S_s}[\hat{n}'\times\bar{E}(\bar{R}')]\centerdot[\frac{jk_0Z_0}{\eta}\hat{n}'\times\bar{\bar{\Gamma}}_W(\bar{R},\bar{R}') - \nabla'\times\bar{\bar{\Gamma}}_W(\bar{R},\bar{R}')]\mathrm{d}s' \tag{3.10}$$

Substituting Eqs. (3.7) and (3.4) into Eq. (3.10) and using the pair relations and orthogonality of the vector wave functions over the segment spherical surface of S_i, we obtain

$$a_q = -\int_{S_S}[\hat{n}'\times\bar{E}(\bar{R}')]\centerdot\bar{A}^{(4)}_q(\bar{R}')\mathrm{d}s' \tag{3.11}$$

$$b_q = -\int_{S_S}[\hat{n}'\times\bar{E}(\bar{R}')]\centerdot\bar{B}^{(4)}_q(\bar{R}')\mathrm{d}s' \tag{3.12}$$

where

$$\bar{A}^{(4)}_q(\bar{R}') = \frac{jk_0Z_0}{\eta}[\hat{n}'\times\bar{M}^{(4)}_{eq}(k_0\bar{R}')] - k_0\bar{N}^{(4)}_{eq}(k_0\bar{R}') \tag{3.13}$$

$$\bar{B}^{(4)}_q(\bar{R}') = \frac{jk_0Z_0}{\eta}[\hat{n}'\times\bar{N}^{(4)}_{oq}(k_0\bar{R}')] - k_0\bar{M}^{(4)}_{oq}(k_0\bar{R}'). \tag{3.14}$$

We can expand $\bar{E}(\bar{R}')$ in terms of spherical vector wave functions as,

$$\bar{E}(\bar{R}') = \sum_{\nu} \left[c_\nu \bar{M}_{e\nu}^{(1)}(k_0 \bar{R}') + d_\nu \bar{N}_{o\nu}^{(1)}(k_0 \bar{R}') \right] \tag{3.15}$$

substituting Eq. (3.15) in Eqs. (3.11) and (3.12), a_q and b_q are found as,

$$a_q = -\sum_{\nu} \int_{S_S} \{ c_\nu [\hat{n}' \times \bar{M}_{e\nu}^{(1)}(k_0 \bar{R}')] \cdot \bar{A}_q^{(4)}(\bar{R}') + d_\nu [\hat{n}' \times \bar{N}_{o\nu}^{(1)}(k_0 \bar{R}')] \cdot \bar{A}_q^{(4)}(\bar{R}') \} \mathrm{d}s' \tag{3.16}$$

$$b_q = -\sum_{\nu} \int_{S_S} \{ c_\nu [\hat{n}' \times \bar{M}_{e\nu}^{(1)}(k_0 \bar{R}')] \cdot \bar{B}_q^{(4)}(\bar{R}') + d_\nu [\hat{n}' \times \bar{N}_{o\nu}^{(1)}(k_0 \bar{R}')] \cdot \bar{B}_q^{(4)}(\bar{R}') \} \mathrm{d}s' \tag{3.17}$$

Eqs. (3.16) and (3.17) can be written in matrix form as follows

$$\begin{bmatrix} a_q \\ b_q \end{bmatrix} = -\begin{bmatrix} Q \end{bmatrix} \begin{bmatrix} c_\nu \\ d_\nu \end{bmatrix} = -\begin{bmatrix} J_{q\nu} & I_{q\nu} \\ L_{q\nu} & K_{q\nu} \end{bmatrix} \begin{bmatrix} c_\nu \\ d_\nu \end{bmatrix} \tag{3.18}$$

where

$$J_{q\nu} = \int_{S_S} [\bar{M}_{e\nu}^{(1)}(k_0 \bar{R}') \times \bar{A}_q^{(4)}(k_0 \bar{R}')] \cdot \hat{n}' \mathrm{d}s' \tag{3.19}$$

$$I_{q\nu} = \int_{S_S} [\bar{N}_{o\nu}^{(1)}(k_0 \bar{R}') \times \bar{A}_q^{(4)}(k_0 \bar{R}')] \cdot \hat{n}' \mathrm{d}s' \tag{3.20}$$

$$L_{q\nu} = \int_{S_S} [\bar{M}_{e\nu}^{(1)}(k_0 \bar{R}') \times \bar{B}_q^{(4)}(k_0 \bar{R}')] \cdot \hat{n}' \mathrm{d}s' \tag{3.21}$$

$$K_{q\nu} = \int_{S_S} [\bar{N}_{o\nu}^{(1)}(k_0 \bar{R}') \times \bar{B}_q^{(4)}(k_0 \bar{R}')] \cdot \hat{n}' \mathrm{d}s'. \tag{3.22}$$

Next consider that $\bar{R}$ is on S_c which is a segment sphere centered at the origin totally outside of the scatterer, and $\bar{R}'$ on S_S. Since $\bar{R}$ is positioned outside of the scatterer, Eq. (3.3) becomes

$$\bar{E}^s(\bar{R}') = \int_{S_S} [\hat{n}' \times \bar{E}(\bar{R}')] \cdot [\frac{jk_0 Z_0}{\eta} \hat{n}' \times \bar{\bar{\Gamma}}_W(\bar{R}, \bar{R}') - \nabla' \times \bar{\bar{\Gamma}}_W(\bar{R}, \bar{R}')] \mathrm{d}s' \tag{3.23}$$

where impedance boundary condition is also applied. Considering that $r > r'$ dyadic Green's function of the wedge can be written as

$$\bar{\bar{\Gamma}}_W(\bar{R}, \bar{R}') = \sum_{q} R_q [\bar{M}_{eq}^{(4)}(k_0 \bar{R}) \bar{M}_{eq}^{(1)}(k_0 \bar{R}') + \bar{N}_{oq}^{(4)}(k_0 \bar{R}) \bar{N}_{oq}^{(1)}(k_0 \bar{R}')]. \tag{3.24}$$

Substituting Eqs. (3.24) and (3.6) in Eq. (3.23) and using the orthogonality of the vector wave functions over the spherical surface of S_c, we have

$$e_p = -\int_{S_S} [\hat{n}' \times \bar{E}(\bar{R}')] \centerdot \bar{A}_p^{(1)}(\bar{R}') \mathrm{d}s' \tag{3.25}$$

$$f_p = -\int_{S_S} [\hat{n}' \times \bar{E}(\bar{R}')] \centerdot \bar{B}_p^{(1)}(\bar{R}') \mathrm{d}s' \tag{3.26}$$

where

$$\bar{A}_p^{(1)}(\bar{R}') = \frac{jk_0 Z_0}{\eta} [\hat{n}' \times \bar{M}_{ep}^{(1)}(k_0 \bar{R}')] - k_0 \bar{N}_{ep}^{(1)}(k_0 \bar{R}') \tag{3.27}$$

$$\bar{B}_p^{(1)}(\bar{R}') = \frac{jk_0 Z_0}{\eta} [\hat{n}' \times \bar{N}_{op}^{(1)}(k_0 \bar{R}')] - k_0 \bar{M}_{op}^{(1)}(k_0 \bar{R}'). \tag{3.28}$$

Using the expansion given in Eq. (3.15) for $\bar{E}(\bar{R}')$, coefficients can be found as

$$e_p = -\sum_{\nu} \int_{S_S} \{c_\nu [\hat{n}' \times \bar{M}_{e\nu}^{(1)}(k_0 \bar{R}')] + d_\nu [\hat{n}' \times \bar{N}_{o\nu}^{(1)}(k_0 \bar{R}')] \centerdot \bar{A}_p^{(1)}(\bar{R}')\} \mathrm{d}s' \tag{3.29}$$

$$f_p = -\sum_{\nu} \int_{S_S} \{c_\nu [\hat{n}' \times \bar{M}_{e\nu}^{(1)}(k_0 \bar{R}')] + d_\nu [\hat{n}' \times \bar{N}_{o\nu}^{(1)}(k_0 \bar{R}')] \centerdot \bar{B}_p^{(1)}(\bar{R}')\}\} \mathrm{d}s' \tag{3.30}$$

Eqs. (3.29) and (3.30) are expressed in matrix form as follows,

$$\begin{bmatrix} e_p \\ f_p \end{bmatrix} = -\begin{bmatrix} Q_e \end{bmatrix} \begin{bmatrix} c_\nu \\ d_\nu \end{bmatrix} = -\begin{bmatrix} J'_{p\nu} & I'_{p\nu} \\ L'_{p\nu} & K'_{p\nu} \end{bmatrix} \begin{bmatrix} c_\nu \\ d_\nu \end{bmatrix} \tag{3.31}$$

where

$$J'_{p\nu} = \int_{S_S} [\bar{M}_{e\nu}^{(1)}(k_0 \bar{R}') \times \bar{A}_p^{(1)}(k_0 \bar{R}')] \centerdot \hat{n}' \mathrm{d}s' \tag{3.32}$$

$$I'_{p\nu} = \int_{S_S} [\bar{N}_{o\nu}^{(1)}(k_0 \bar{R}') \times \bar{A}_p^{(1)}(k_0 \bar{R}')] \centerdot \hat{n}' \mathrm{d}s' \tag{3.33}$$

$$L'_{p\nu} = \int_{S_S} [\bar{M}_{e\nu}^{(1)}(k_0 \bar{R}') \times \bar{B}_p^{(1)}(k_0 \bar{R}')] \centerdot \hat{n}' \mathrm{d}s' \tag{3.34}$$

$$K'_{q\nu} = \int_{S_S} [\bar{N}_{o\nu}^{(1)}(k_0 \bar{R}') \times \bar{B}_p^{(1)}(k_0 \bar{R}')] \centerdot \hat{n}' \mathrm{d}s'. \tag{3.35}$$

Using Eqs. (3.18) and (3.31), we can relate the scattered field coefficients to the incident field coefficients in matrix form as

$$\begin{bmatrix} e_p \\ f_p \end{bmatrix} = \Big[T\Big] \begin{bmatrix} a_q \\ b_q \end{bmatrix} \tag{3.36}$$

where the T-matrix is defined as

$$\Big[T\Big] = -\Big[Q_e\Big]\Big[Q\Big]^{-1} \tag{3.37}$$

Eq. (3.36) shows the relation between the scattered field coefficients and the incident field coefficients which can be calculated using Eqs. (3.1) and (3.4) as,

$$a_q = jk_0 Z_0 \int_{V_j} \bar{M}_{eq}^{(4)}(k_0\bar{R}') \centerdot \bar{J}_v(\bar{R}')\mathrm{d}v' \tag{3.38}$$

$$b_q = jk_0 Z_0 \int_{V_j} \bar{N}_{oq}^{(4)}(k_0\bar{R}') \centerdot \bar{J}_v(\bar{R}')\mathrm{d}v' \tag{3.39}$$

3.2 Comments on the T-matrix

T-matrix elements only depend on the size, shape and composition of the scatterer and also the wedge angle which identifies the eigenvalues. T-matrix is independent of the scattered and incident fields direction and polarization, however, it is unique for all incident field frequencies.

It is efficient to calculate the whole Q-matrix and Q_e-matrix for a given incident wave frequency simultaneously, in this manner, redundant calculation of the Bessel, Hankel and Legendre functions for each point on the scatterer, can be avoided for each matrix element.

Theoretically, the size of the T-matrix is infinite but for numerical evaluation, it should be truncated into a finite size. Proper truncation is influenced by the size of the scatterer and the choice of the origin of coordinates. For better convergence, size of the object should be kept small and the origin should be at the center of the symmetry. For large and elongated objects where the ratio

of the radii of circumscribing sphere to inscribing sphere is large, higher order terms are needed in the T-matrix. This resulting matrix is ill-conditioned which is impractical to invert numerically. Computation of the T-matrix is discussed in detail in [17].

3.3 Verification of the T-Matrix

We analytically verify T-matrix method by employing it for a spherical impedance boss centered at the edge. Then, results are compared with the one obtained from dyadic Green's function solution. To this aim, a spherical scatterer centered at the origin with radius a is considered. Since the surface is spherical, orthogonality relations of auxiliary vector wave functions (see Appendix A) can be utilized. Q-matrix elements is calculated as

$$\begin{aligned} J_{q\nu} &= k_0 z_q^{(1)}(k_0 r)\,\{\frac{1}{\kappa}k_0 h_{\mu+n}^{(2)}(k_0 r) - \frac{k_0}{r}\frac{d}{dr}[r h_{\mu+n}^{(2)}(k_0 r)]\}\Big|_{r=a} \\ &\quad \frac{2Q_{\mu n}(\mu+n)(\mu+n+1)}{\pi}\delta_{\mu\mu'}\delta_{nn'} \qquad (3.40) \\ I_{q\nu} &= 0 \qquad (3.41) \\ L_{q\nu} &= 0 \qquad (3.42) \\ K_{q\nu} &= \frac{1}{r}\frac{d}{dr}[r j_{\mu+n}(k_0 r)]\,\{\frac{1}{\kappa}\frac{1}{r}\frac{d}{dr}[r h_{\mu+n}^{(2)}(k_0 r)] + k_0^2 h_{\mu+n}^{(2)}(k_0 r)\}\Big|_{r=a} \\ &\quad \frac{2Q_{\mu n}(\mu+n)(\mu+n+1)}{\pi}\delta_{\mu\mu'}\delta_{nn'} \qquad (3.43) \end{aligned}$$

and for $[Q_e]$ is found to be

$$\begin{aligned} J'_{q\nu} &= k_0 j_{\mu+n}(k_0 r)\,\{\frac{1}{\kappa}k_0 j_{\mu+n}(k_0 r) - \frac{k_0}{r}\frac{d}{dr}[r j_{\mu+n}(k_0 r)]\}\Big|_{r=a} \\ &\quad \frac{2Q_{\mu n}(\mu+n)(\mu+n+1)}{\pi}\delta_{\mu\mu'}\delta_{nn'} \qquad (3.44) \\ I'_{q\nu} &= 0 \qquad (3.45) \\ L'_{q\nu} &= 0 \qquad (3.46) \\ K'_{q\nu} &= \frac{1}{r}\frac{d}{dr}[r j_{\mu+n}(k_0 r)]\,\{\frac{1}{\kappa}\frac{1}{r}\frac{d}{dr}[r j_{\mu+n}(k_0 r)] + k_0^2 j_{\mu+n}(k_0 r)\}\Big|_{r=a} \\ &\quad \frac{2Q_{\mu n}(\mu+n)(\mu+n+1)}{\pi}\delta_{\mu\mu'}\delta_{nn'} \qquad (3.47) \end{aligned}$$

It is seen that both $[Q]$ and $[Q_e]$ are diagonal matrices, consequently, according to Eq. (3.37), T-matrix is diagonal too. Substituting these elements in Eq. (3.36) and performing the matrix operations we obtain,

$$\begin{aligned} e_q &= -\frac{(\frac{1}{\kappa}-\frac{1}{a})j_{\mu+n}(k_0a)-k_0j'_{\mu+n}(k_0a)}{(\frac{1}{\kappa}-\frac{1}{a})h^{(2)}_{\mu+n}(k_0a)-k_0^2h^{(2)'}_{\mu+n}(k_0a)}a_q \\ &= -\frac{k_0\kappa j'_{\mu+n}(k_0a)+(\frac{\kappa}{a}-1)j_{\mu+n}(k_0a)}{k_0\kappa h^{(2)\prime}_{\mu+n}(k_0a)+(\frac{\kappa}{a}-1)h^{(2)}_{\mu+n}(k_0a)}a_q \end{aligned} \tag{3.48}$$

$$\begin{aligned} f_q &= -\frac{\frac{k_0}{\kappa}j'_{\mu+n}(k_0a)+\frac{1}{\kappa a}+k_0^2j_{\mu+n}(k_0a)}{\frac{k_0}{\kappa}h^{(2)'}_{\mu+n}(k_0a)+\frac{1}{\kappa a}+k_0^2h^{(2)}_{\mu+n}(k_0a)} \\ &= -\frac{k_0j'_{\mu+n}(k_0a)+(\frac{1}{a}+k_0^2\kappa)j_{\mu+n}(k_0a)}{k_0h^{(2)\prime}_{\mu+n}(k_0a)+(\frac{1}{a}+k_0^2\kappa)h^{(2)}_{\mu+n}(k_0a)}b_q \end{aligned} \tag{3.49}$$

Coefficients relating e_q to a_q in Eq. (3.48) are identical to $\alpha_{\mu n}(k_0a)$ which is given in Eq. (2.39). Similarly, coefficients in Eq. (3.49) are same as $\beta_{\mu n}(k_0a)$ defined in Eq. (2.40). Scattered field coefficients can be found by substituting Eqs. (3.38) and (3.39) in Eqs. (3.48) and (3.49). The resulting expression will be

$$e_q = jk_0Z_0\alpha_{\mu n}(k_0a)\int\limits_{V_j}\bar{M}^{(4)}_{eq}(k_0\bar{R}')\centerdot\bar{J}_v(\bar{R}')\mathrm{d}v' \tag{3.50}$$

$$f_q = jk_0Z_0\beta_{\mu n}(k_0a)\int\limits_{V_j}\bar{N}^{(4)}_{oq}(k_0\bar{R}')\centerdot\bar{J}_v(\bar{R}')\mathrm{d}v' \tag{3.51}$$

Scattered field is calculated using Eq. (3.6) as follows

$$\begin{aligned} \bar{E}^s(\bar{R}) &= jk_0Z_0\sum_q\frac{j\pi}{2k_0(\mu+n)(\mu+n+1)Q_{\mu n}} \\ &\cdot\ [\alpha_{\mu n}(k_0a)\bar{M}^{(4)}_{eq}(k_0\bar{R})\int\limits_{V_j}\bar{M}^{(4)}_{eq}(k_0\bar{R}')\centerdot\bar{J}_v(\bar{R}')\mathrm{d}v' \\ &+\ \beta_{\mu n}(k_0a)\bar{N}^{(4)}_{oq}(k_0\bar{R})\int\limits_{V_j}\bar{N}^{(4)}_{oq}(k_0\bar{R}')\centerdot\bar{J}_v(\bar{R}')\mathrm{d}v'] \end{aligned} \tag{3.52}$$

which is identical to the result given in (2.86) i.e.

$$\bar{E}^s(\bar{R}) = jk_0Z_0\int\limits_{V_j}\bar{\bar{\Gamma}}_B(\bar{R},\bar{R}')\centerdot\bar{J}_v(\bar{R}')dv' \tag{3.53}$$

where $\bar{\bar{\Gamma}}_B(\bar{R}, \bar{R}')$ is the dyadic Green's function of the boss given in Eq. (2.83). This result indicates that the T-matrix method and dyadic Green's function solution are in perfect agreement for a spherical scatterer.

To verify the T-matrix for an irregularly shaped object, once more the spherical scatterer can be used but this time its center is placed off the origin. Since the wedge is extended to infinity, scattered field should be equal to the field calculated using the dyadic Green's function where the center is assumed at origin. In this case there is no spherical symmetry with respect to the origin, as a result, off-diagonal components of the $[Q]$ and $[Q_e]$ are non zero.

Geometry of the problem is depicted in Fig. 3.2 where the spherical boss of radius $a = 0.25\lambda$ is placed at $z = 0.1\lambda$ and impedance of the boss is assumed as $\eta = 1.5Z_0$. The mono-static scattered field is plotted in Figs. 3.3 – 3.8 and the

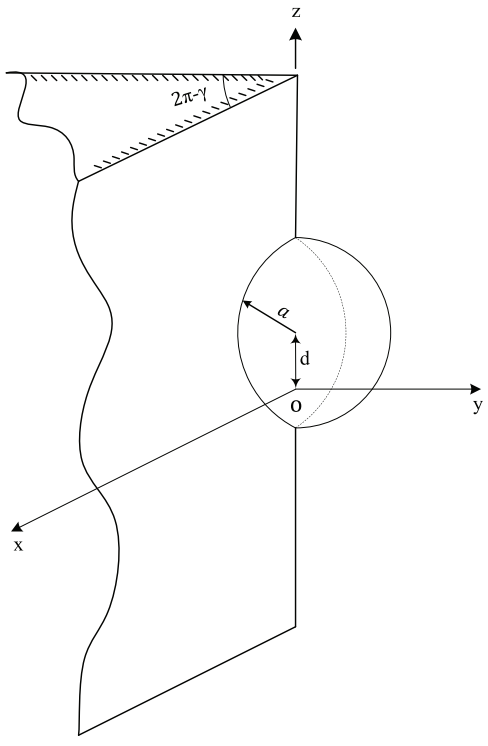

Figure 3.2: Geometry of the shifted spherical scatterer at the edge

results are compared with the one obtained from dyadic Green's function (DGF) solution. Excellent agreement is achieved between two methods.

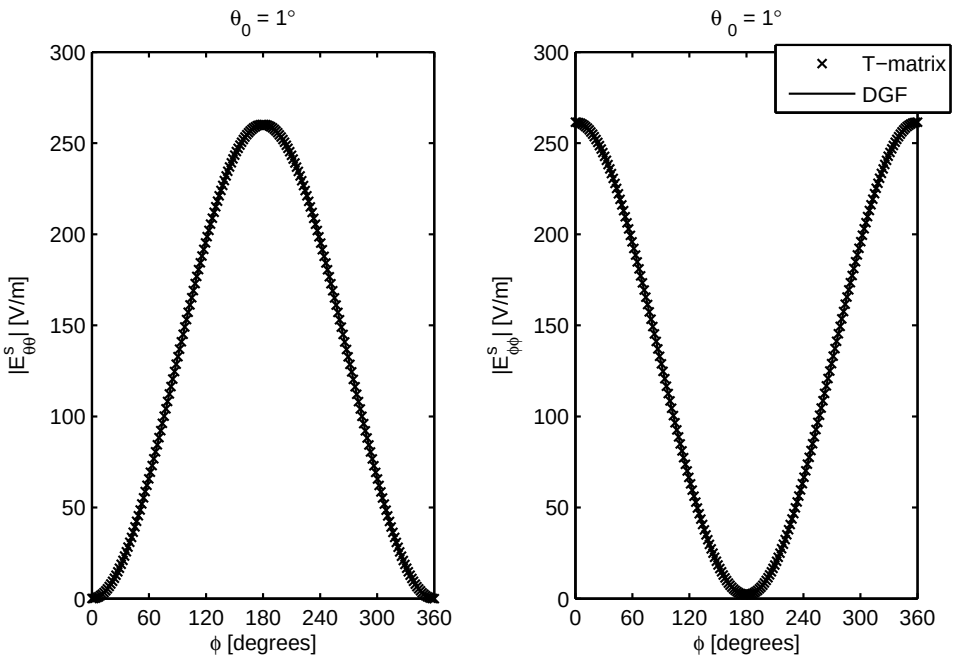

Figure 3.3: Comparison of T-matrix and DGF methods for the monostatic scattered field pattern for $a = 0.25\lambda$, $\gamma = 2\pi$, $\theta_0 = 1^\circ$ and $\eta = 1.5Z_0$. T-matrix solution is obtained for a sphere shifted by $d = 0.1\lambda$.

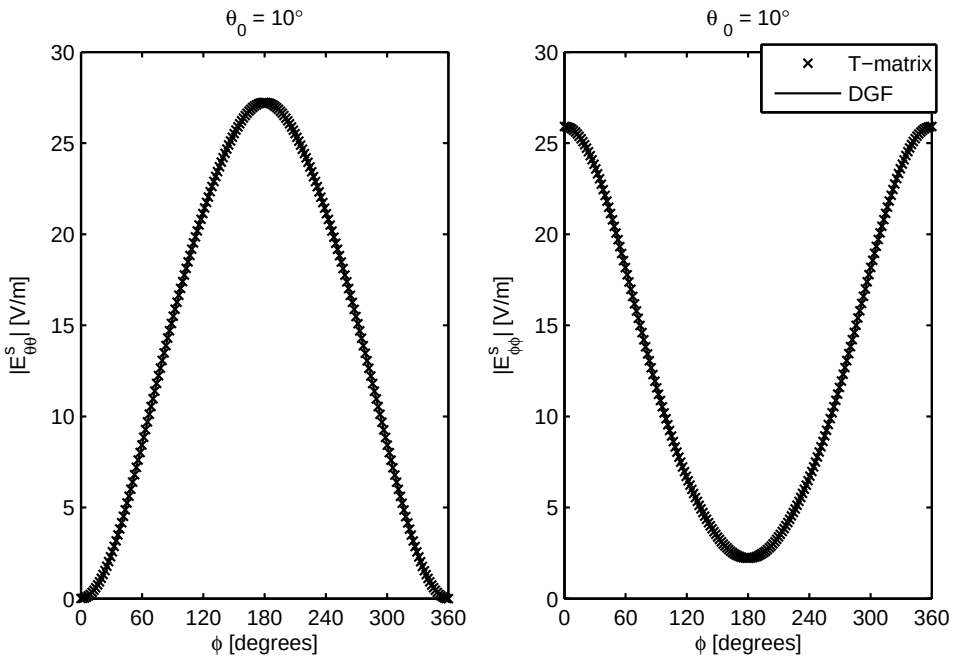

Figure 3.4: Comparison of T-matrix and DGF methods for the monostatic scattered field pattern for $a = 0.25\lambda$, $\gamma = 2\pi$, $\theta_0 = 10^\circ$ and $\eta = 1.5Z_0$. T-matrix solution is obtained for a sphere shifted by $d = 0.1\lambda$.

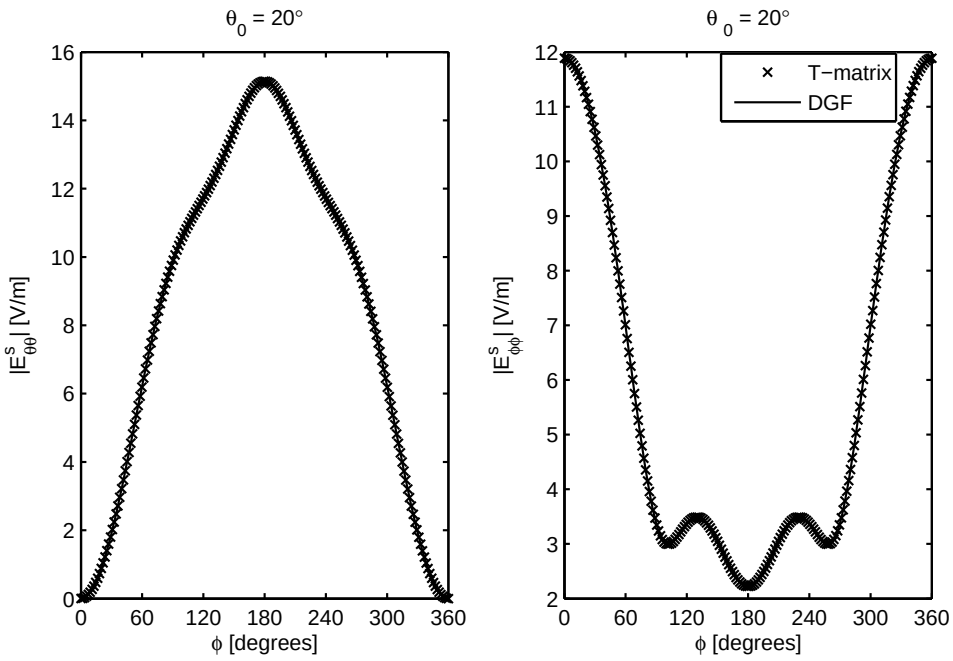

Figure 3.5: Comparison of T-matrix and DGF methods for the monostatic scattered field pattern for $a = 0.25\lambda$, $\gamma = 2\pi$, $\theta_0 = 20^\circ$ and $\eta = 1.5Z_0$. T-matrix solution is obtained for a sphere shifted by $d = 0.1\lambda$.

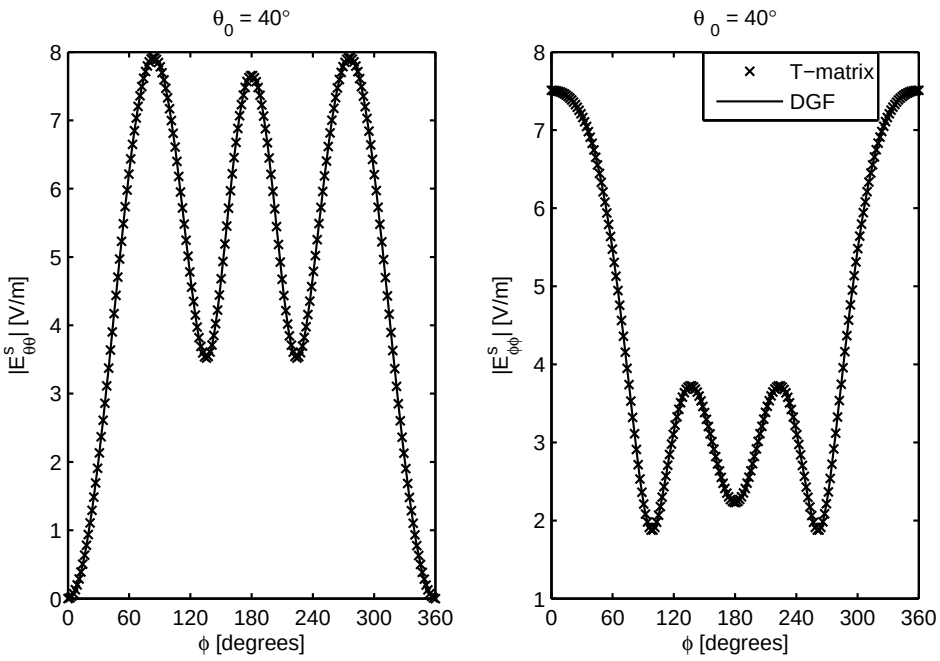

Figure 3.6: Comparison of T-matrix and DGF methods for the monostatic scattered field pattern for $a = 0.25\lambda$, $\gamma = 2\pi$, $\theta_0 = 40^\circ$ and $\eta = 1.5Z_0$. T-matrix solution is obtained for a sphere shifted by $d = 0.1\lambda$.

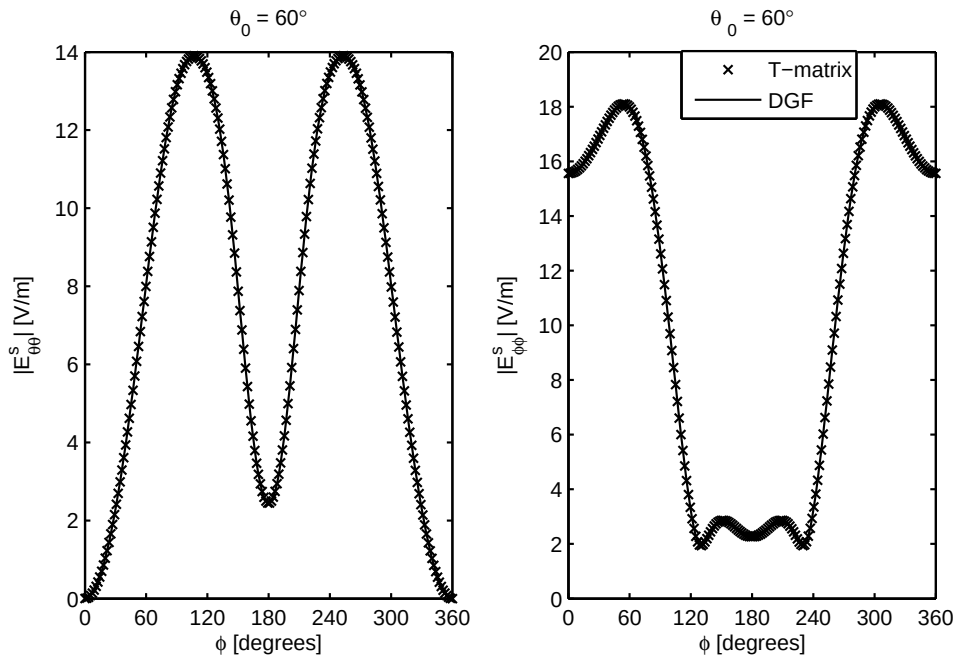

Figure 3.7: Comparison of T-matrix and DGF methods for the monostatic scattered field pattern for $a = 0.25\lambda$, $\gamma = 2\pi$, $\theta_0 = 60^\circ$ and $\eta = 1.5Z_0$. T-matrix solution is obtained for a sphere shifted by $d = 0.1\lambda$.

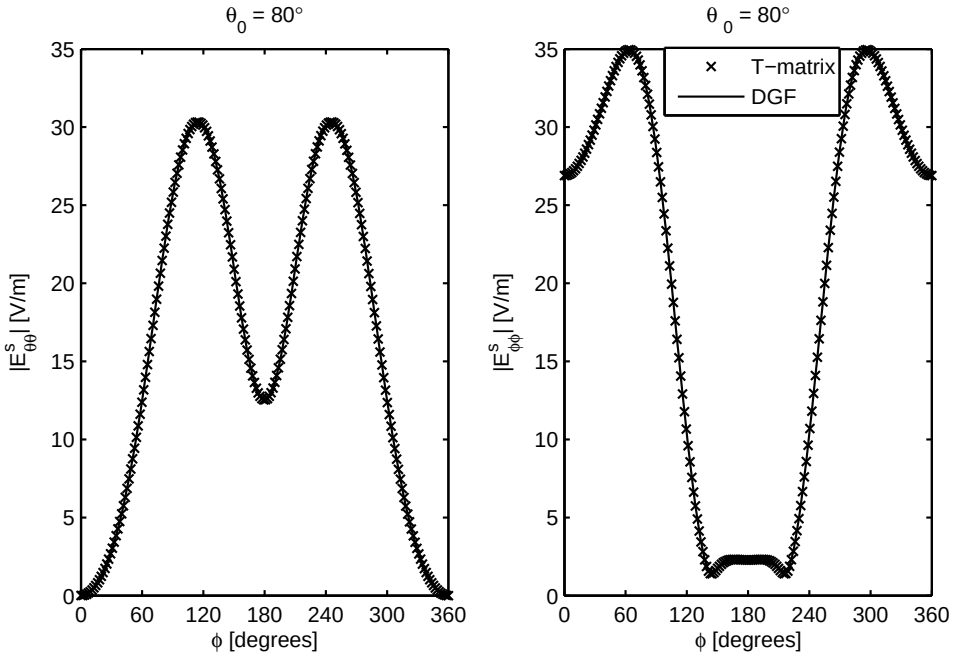

Figure 3.8: Comparison of T-matrix and DGF methods for the monostatic scattered field pattern for $a = 0.25\lambda$, $\gamma = 2\pi$, $\theta_0 = 80^\circ$ and $\eta = 1.5Z_0$. T-matrix solution is obtained for a sphere shifted by $d = 0.1\lambda$.

Chapter 4

Multiple Scatterers at the Edge

This chapter is concerned with the scattering form multiple objects at the edge. Unlike the previous chapter where only the effect of the wedge on the scatterer is considered, here mutual interaction of the scatterers is also included. Therefore, incident field on each scatterer consists of two parts: First, the field in the presence of the wedge (as defined in Chapter 3). Second, the scattered field from other objects. Mutual interaction between scatterers are taken into account by introducing two Q-matirces. The procedure followed here is an extension of the one outlined in [7].

In the following subsections, first, basic case of two scatterers at the edge is considered and T-matrix formulation is developed. Then, the solution is generalized for multiple scatterers.

4.1 T-matrix Formulation for Two Scatterers

Consider the Geometry of Fig. 4.1 which two impedance scatterers are situated at the edge of a PEC wedge which extends to infinity along z-axis. Two spherical coordinates are defined where their origins O_1 and O_2 are positioned along the z-axis with a separation distance of d. O_1 and O_2 are situated inside the scatterer

1 and the scatterer 2, respectively. A position in the first coordinates is denoted by $\bar{R}_1$ which represents r_1, θ_1 and ϕ. The same position is defined in second coordinates by $\bar{R}_2$ (r_2, θ_2, ϕ). In order to apply the T-matrix, the smallest sphere which circumscribe each scatterer should not overlap. In addition, sources should be outside the scatterers and be farther from each scatterer by at least d.

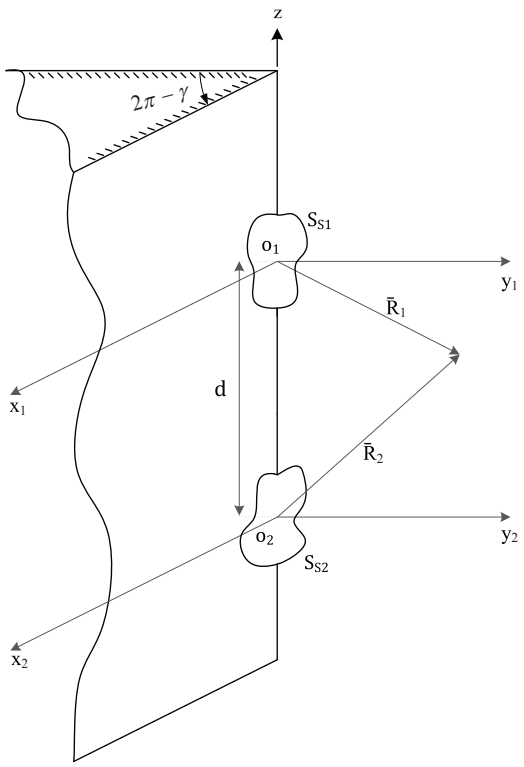

Figure 4.1: Two scatterers at the edge of a wedge

The field in presence of the wedge is denoted as $\bar{E}^0$ which is incident on scatterers 1 and 2. $\bar{E}^0$ can be expanded in terms of spherical vector wave functions in both coordinates as follows

$$\bar{E}^0(\bar{R}_1) = \sum_q R_q[a_q^1 \bar{M}_{eq}^{(1)}(k_0\bar{R}_1) + b_q^1 \bar{N}_{oq}^{(1)}(k_0\bar{R}_1)] \tag{4.1}$$

$$\bar{E}^0(\bar{R}_2) = \sum_q R_q[a_q^2 \bar{M}_{eq}^{(1)}(k_0\bar{R}_2) + b_q^2 \bar{N}_{oq}^{(1)}(k_0\bar{R}_2)] \tag{4.2}$$

where a_q^1, a_q^2, b_q^1 and b_q^2 are coefficients which are assumed to be known. R_q as

defined as in Eq. (3.5) is

$$R_q = \frac{j\pi}{2k_0(\mu+n)(\mu+n+1)Q_{\mu n}}. \tag{4.3}$$

Incident field on the scatterers is the sum of $\bar{E}^0$ and the field scattered by the other scatterer. Thus we can write,

$$\bar{E}_1^i(\bar{R}_1) = \sum_q R_q \left[(a_q^1 + g_q^{12})\bar{M}_{eq}^{(1)}(k_0\bar{R}_1) + (b_q^1 + h_q^{12})\bar{N}_{oq}^{(1)}(k_0\bar{R}_1)\right] \tag{4.4}$$

$$\bar{E}_2^i(\bar{R}_2) = \sum_q R_q \left[(a_q^2 + g_q^{21})\bar{M}_{eq}^{(1)}(k_0\bar{R}_2) + (b_q^2 + h_q^{21})\bar{N}_{oq}^{(1)}(k_0\bar{R}_2)\right] \tag{4.5}$$

where g_q^{12} and h_q^{12} are coefficients of the field scattered from object 2 incident on object 1. Similarly, g_q^{21} and h_q^{21} are the coefficients of the field scattered from object 1 incident on object 2. These coefficients include the effect of the all multiple scattering from scatterers 1 and 2.

The next step is to apply the Green's second identity on the inscribing spheres of two scatterers which is similar to the procedure followed in Chapter 3. Applying Green's identity (see Eq. (3.3)) and considering $\bar{R}_1$ on inscribing sphere of scatterer 1 and $\bar{R}_1'$ on the scatterer 1 we have,

$$-\bar{E}_1^i(\bar{R}_1) = \int_{S_{S_1}} \{-\bar{\bar{\Gamma}}_W(\bar{R}_1, \bar{R}_1')\centerdot[\hat{n}_1' \times \nabla_1' \times \bar{E}(\bar{R}_1')] - [\hat{n}_1' \times \bar{E}(\bar{R}_1')]\centerdot[\nabla_1' \times \bar{\bar{\Gamma}}_W(\bar{R}_1, \bar{R}_1')]\}\mathrm{d}s' \tag{4.6}$$

where n_1' and $\nabla_1'\times$ is the unit normal vector and curl operation in the first coordinates, respectively. Note that according to the boundary conditions, surface integration is only limited to the surface of the scatterer 1, S_{S_1} (see Chapter 3).

Imposing the impedance boundary condition on the surface of the scatterer 1, Eq. (4.6) becomes

$$-\bar{E}^i(\bar{R}_1) = \int_{S_{S1}} [\hat{n}_1' \times \bar{E}(\bar{R}_1')]\centerdot[\frac{jk_0Z_0}{\eta_1}\hat{n}_1' \times \bar{\bar{\Gamma}}_W(\bar{R}_1, \bar{R}_1') - \nabla_1' \times \bar{\bar{\Gamma}}_W(\bar{R}_1, \bar{R}_1')]\mathrm{d}s' \tag{4.7}$$

where η_1 is the surface impedance of the scatterer 1. Using Eq. (4.4) and explicit expression for $\bar{\bar{\Gamma}}_W$(Eq. (2.82)) considering $r < r'$ and applying the orthogonality

of the vector wave functions over the segment inscribing sphere of scatterer 1, we obtain,

$$a_q^1 + g_q^{12} = \int_{S_{S1}} [\hat{n}_1' \times \bar{E}(\bar{R}_1')] \cdot \bar{A}_q^{1(4)} \mathrm{d}s' \tag{4.8}$$

$$b_q^1 + h_q^{12} = \int_{S_{S1}} [\hat{n}_1' \times \bar{E}(\bar{R}_1')] \cdot \bar{B}_q^{1(4)} \mathrm{d}s' \tag{4.9}$$

where

$$\bar{A}_q^{1(4)} = \frac{jk_0 Z_0}{\eta_1} [\hat{n}_1' \times \bar{M}_{eq}^{(4)}(k_0 \bar{R}_1')] - k_0 \bar{N}_{eq}^{(4)}(k_0 \bar{R}_1') \tag{4.10}$$

and

$$\bar{B}_q^{1(4)} = \frac{jk_0 Z_0}{\eta_1} [\hat{n}_1' \times \bar{N}_{oq}^{(4)}(k_0 \bar{R}_1')] - k_0 \bar{M}_{oq}^{(4)}(k_0 \bar{R}_1') \tag{4.11}$$

Total electric field intensity on the surface of the scatterer 1 can be expanded in terms of spherical vector wave functions as

$$\bar{E}(\bar{R}_1) = \sum_{\nu} c_\nu^1 \bar{M}_{e\nu}^{(1)}(k_0 \bar{R}_1) + d_\nu^1 \bar{N}_{o\nu}^{(1)}(k_0 \bar{R}_1) \tag{4.12}$$

Substituting Eq. (4.12) in Eqs. (4.8) and (4.9) we relate the unknown coefficients of c_ν^1 and d_ν^1 to the incident field coefficients. This relation can be written in matrix form as

$$\begin{bmatrix} a_q^1 + g_q^{12} \\ b_q^1 + h_q^{12} \end{bmatrix} = - \left[Q_{q\nu}^1 \right] \begin{bmatrix} c_\nu^1 \\ d_\nu^1 \end{bmatrix} \tag{4.13}$$

The $[Q^1]$ matrix is partitioned as

$$\left[Q_{q\nu}^1 \right] = \begin{bmatrix} J_{q\nu}^1 & I_{q\nu}^1 \\ L_{q\nu}^1 & K_{q\nu}^1 \end{bmatrix} \tag{4.14}$$

where

$$J_{q\nu}^1 = \int_{S_{S_1}} [\bar{M}_{e\nu}^{(1)}(k_0 \bar{R}_1') \times \bar{A}_q^{1(4)}] \cdot \hat{n}_1' \mathrm{d}s' \tag{4.15}$$

$$I_{q\nu}^1 = \int_{S_{S_1}} [\bar{N}_{o\nu}^{(1)}(k_0 \bar{R}_1') \times \bar{A}_q^{1(4)}] \cdot \hat{n}_1' \mathrm{d}s' \tag{4.16}$$

$$L_{q\nu}^1 = \int_{S_{S_1}} [\bar{M}_{e\nu}^{(1)}(k_0 \bar{R}_1') \times \bar{B}_q^{1(4)}] \cdot \hat{n}_1' \mathrm{d}s' \tag{4.17}$$

$$K^1_{q\nu} = \int\limits_{S_{S_1}} [\bar{N}^{(1)}_{o\nu}(k_0\bar{R}'_1) \times \bar{B}^{1(4)}_q] \centerdot \hat{n}'_1 \mathrm{d}s' \tag{4.18}$$

If we apply the Green's second identity assuming that $\bar{R}_1$ is on scatterer 2, scattered field form scatterer 1 can be written as

$$\bar{E}^s_1(\bar{R}_2) = \int\limits_{S_{S1}} [\hat{n}'_1 \times \bar{E}(\bar{R}'_1)] \centerdot [\frac{jk_0Z_0}{\eta}\hat{n}'_1 \times \bar{\bar{\Gamma}}_W(\bar{R}_2, \bar{R}'_2) - \nabla'_1 \times \bar{\bar{\Gamma}}_W(\bar{R}_2, \bar{R}'_2)]\mathrm{d}s' \tag{4.19}$$

Note that dyadic Green's function of the wedge is expressed in the second coordinates for further simplification of the expressions.

As mentioned earlier incident field on the scatterer 2 can be written as,

$$\bar{E}^i_2(\bar{R}_2) = \bar{E}^0(\bar{R}_2) + \bar{E}^s_1(\bar{R}_2) \tag{4.20}$$

Substituting Eqs. (4.2) and (4.5) in Eq. (4.20) we obtain,

$$\begin{aligned} \bar{E}^s_1(\bar{R}_2) &= \bar{E}^i_2(\bar{R}_2) - \bar{E}^0(\bar{R}_2) \\ &= \sum_q R_q[g^{21}_q \bar{M}^{(1)}_{eq}(k_0\bar{R}_2) + h^{21}_q \bar{N}^{(1)}_{oq}(k_0\bar{R}_2)] \end{aligned} \tag{4.21}$$

If we place Eq. (4.19) in Eq. (4.21) and use the orthogonality of the vector wave functions, we obtain,

$$g^{21}_q = \int\limits_{S_{S1}} [\hat{n}'_1 \times \bar{E}(\bar{R}'_1)] \centerdot \bar{G}^{21}_q \mathrm{d}s' \tag{4.22}$$

$$h^{21}_q = \int\limits_{S_{S1}} [\hat{n}'_1 \times \bar{E}(\bar{R}'_1)] \centerdot \bar{H}^{21}_q \mathrm{d}s' \tag{4.23}$$

where

$$\bar{G}^{21}_q = \frac{jk_0Z_0}{\eta_1}[\hat{n}'_1 \times \bar{M}^{(4)}_{eq}(k_0\bar{R}'_2)] - \nabla'_1 \times \bar{M}^{(4)}_{eq}(k_0\bar{R}'_2) \tag{4.24}$$

$$\bar{H}^{21}_q = \frac{jk_0Z_0}{\eta_1}[\hat{n}'_1 \times \bar{N}^{(4)}_{oq}(k_0\bar{R}'_2)] - \nabla'_1 \times \bar{N}^{(4)}_{oq}(k_0\bar{R}'_2). \tag{4.25}$$

By substituting Eq. (4.12) is Eqs. (4.22) and (4.23), following matrix equation can be obtained,

$$\begin{bmatrix} g^{21}_q \\ h^{21}_q \end{bmatrix} = \begin{bmatrix} Q^{21}_{q\nu} \end{bmatrix} \begin{bmatrix} c^1_\nu \\ d^1_\nu \end{bmatrix} \tag{4.26}$$

where

$$\left[Q_{q\nu}^{21}\right] = \begin{bmatrix} J_{q\nu}^{21} & I_{q\nu}^{21} \\ L_{q\nu}^{21} & K_{q\nu}^{21} \end{bmatrix} \tag{4.27}$$

with

$$J_{q\nu}^{21} = \int\limits_{S_{S_1}} [\bar{M}_{e\nu}^{(1)}(k_0\bar{R}_1') \times \bar{G}_q^{21}] \centerdot \hat{n}_1' \mathrm{d}s' \tag{4.28}$$

$$I_{q\nu}^{21} = \int\limits_{S_{S_1}} [\bar{N}_{o\nu}^{(1)}(k_0\bar{R}_1') \times \bar{G}_q^{21}] \centerdot \hat{n}_1' \mathrm{d}s' \tag{4.29}$$

$$L_{q\nu}^{21} = \int\limits_{S_{S_1}} [\bar{M}_{e\nu}^{(1)}(k_0\bar{R}_1') \times \bar{H}_q^{21}] \centerdot \hat{n}_1' \mathrm{d}s' \tag{4.30}$$

$$K_{q\nu}^{21} = \int\limits_{S_{S_1}} [\bar{N}_{o\nu}^{(1)}(k_0\bar{R}_1') \times \bar{H}_q^{21}] \centerdot \hat{n}_1' \mathrm{d}s'. \tag{4.31}$$

The steps followed through Eq. (4.6) to (4.31) are repeated again but this time for the scatterer 2. Using Eqs. (3.3) and (4.5) and considering the following expansion for the total field on the surface of scatterer 2,

$$\bar{E}(\bar{R}_2) = \sum_{\nu} c_\nu^2 \bar{M}_{e\nu}^{(1)}(k_0\bar{R}_2) + d_\nu^2 \bar{N}_{o\nu}^{(1)}(k_0\bar{R}_2) \tag{4.32}$$

one could obtain the following matrix relation between coefficients of $\bar{E}_2^i$ and c_ν^2, d_ν^2 as

$$\begin{bmatrix} a_q^2 + g_q^{21} \\ b_q^2 + h_q^{21} \end{bmatrix} = -\left[Q_{q\nu}^2\right] \begin{bmatrix} c_\nu^2 \\ d_\nu^2 \end{bmatrix} \tag{4.33}$$

Q-matrix for scatterer 2, $[Q^2]$, is partitioned as,

$$\left[Q_{q\nu}^2\right] = \begin{bmatrix} J_{q\nu}^2 & I_{q\nu}^2 \\ L_{q\nu}^2 & K_{q\nu}^2 \end{bmatrix} \tag{4.34}$$

where

$$J_{q\nu}^2 = \int\limits_{S_{S_2}} [\bar{M}_{e\nu}^{(1)}(k_0\bar{R}_2') \times \bar{A}_q^{2(4)}] \centerdot \hat{n}_2' \mathrm{d}s' \tag{4.35}$$

$$I_{q\nu}^2 = \int\limits_{S_{S_2}} [\bar{N}_{o\nu}^{(1)}(k_0\bar{R}_2') \times \bar{A}_q^{2(4)}] \centerdot \hat{n}_2' \mathrm{d}s' \tag{4.36}$$

$$L^2_{q\nu} = \int\limits_{S_{S_2}} [\bar{M}^{(1)}_{e\nu}(k_0\bar{R}'_2) \times \bar{B}^{2(4)}_q] \cdot \hat{n}'_2 \mathrm{d}s' \tag{4.37}$$

$$K^2_{q\nu} = \int\limits_{S_{S_2}} [\bar{N}^{(1)}_{o\nu}(k_0\bar{R}'_2) \times \bar{B}^{2(4)}_q] \cdot \hat{n}'_2 \mathrm{d}s' \tag{4.38}$$

and

$$\bar{A}^{2(4)}_q = \frac{jk_0Z_0}{\eta_2}[\hat{n}'_2 \times \bar{M}^{(4)}_{eq}(k_0\bar{R}'_2)] - k_0\bar{N}^{(4)}_{eq}(k_0\bar{R}'_2) \tag{4.39}$$

$$\bar{B}^{2(4)}_q = \frac{jk_0Z_0}{\eta_2}[\hat{n}'_2 \times \bar{N}^{(4)}_{oq}(k_0\bar{R}'_2)] - k_0\bar{M}^{(4)}_{oq}(k_0\bar{R}'_2) \tag{4.40}$$

$\hat{n}'_2$ is the unit vector normal to the surface of scatterer 2 and η_2 is the surface impedance of the scatterer 2.

Scattered field from scatterer 2 incident on scatterer 1 is written as

$$\bar{E}^s_2(\bar{R}_1) = \int\limits_{S_{S_2}} [\hat{n}'_2 \times \bar{E}(\bar{R}'_2)] \cdot [\frac{jk_0Z_0}{\eta_2}\hat{n}'_2 \times \bar{\bar{\Gamma}}_W(\bar{R}_1, \bar{R}'_1) - \nabla'_2 \times \bar{\bar{\Gamma}}_W(\bar{R}_1, \bar{R}'_1)]\mathrm{d}s' \tag{4.41}$$

where ∇'_2 denotes the curl operation in the second coordinates. Again, using Green's second identity (Eq.(3.3)) and Eq. (4.5), similar to Eq. (4.26) one could obtain

$$\begin{bmatrix} g^{12}_q \\ h^{12}_q \end{bmatrix} = \begin{bmatrix} Q^{12}_{q\nu} \end{bmatrix} \begin{bmatrix} c^2_\nu \\ d^2_\nu \end{bmatrix} \tag{4.42}$$

$[Q^{12}]$ is defined as follows

$$\begin{bmatrix} Q^{12}_{q\nu} \end{bmatrix} = \begin{bmatrix} J^{12}_{q\nu} & I^{12}_{q\nu} \\ L^{12}_{q\nu} & K^{12}_{q\nu} \end{bmatrix} \tag{4.43}$$

where

$$J^{12}_{q\nu} = \int\limits_{S_{S_2}} [\bar{M}^{(1)}_{e\nu}(k_0\bar{R}'_2) \times \bar{G}^{12}_q] \cdot \hat{n}'_2 \mathrm{d}s' \tag{4.44}$$

$$I^{12}_{q\nu} = \int\limits_{S_{S_2}} [\bar{N}^{(1)}_{o\nu}(k_0\bar{R}'_2) \times \bar{G}^{12}_q] \cdot \hat{n}'_2 \mathrm{d}s' \tag{4.45}$$

$$L^{12}_{q\nu} = \int\limits_{S_{S_2}} [\bar{M}^{(1)}_{e\nu}(k_0\bar{R}'_2) \times \bar{H}^{12}_q] \cdot \hat{n}'_2 \mathrm{d}s' \tag{4.46}$$

$$K^{12}_{q\nu} = \int\limits_{S_{S_2}} [\bar{N}^{(1)}_{o\nu}(k_0\bar{R}'_2) \times \bar{H}^{12}_q] \cdot \hat{n}'_2 \mathrm{d}s'. \tag{4.47}$$

with

$$\bar{G}_q^{12} = \frac{jk_0 Z_0}{\eta_2}[\hat{n}_2' \times \bar{M}_{eq}^{(4)}(k_0 \bar{R}_1')] - \nabla_2' \times \bar{M}_{eq}^{(4)}(\bar{R}_1') \tag{4.48}$$

$$\bar{H}_q^{12} = \frac{jk_0 Z_0}{\eta_2}[\hat{n}_2' \times \bar{N}_{oq}^{(4)}(k_0 \bar{R}_1')] - \nabla_2' \times \bar{N}_{oq}^{(4)}(\bar{R}_1'). \tag{4.49}$$

In order to find the the electric field on the surface of the scatterer 1, Eq. (4.42) is substituted in Eq. (4.13) which yields,

$$\begin{bmatrix} c_\nu^1 \\ d_\nu^1 \end{bmatrix} = -\left[Q^1\right]^{-1} \begin{bmatrix} a_q^1 \\ b_q^1 \end{bmatrix} + \left[T^{12}\right] \begin{bmatrix} c_\nu^2 \\ d_\nu^2 \end{bmatrix} \tag{4.50}$$

where

$$\left[T^{12}\right] = -\left[Q^1\right]^{-1} \left[Q^{12}\right]. \tag{4.51}$$

Similarly for the coefficients of the total field on scatterer 2 we have,

$$\begin{bmatrix} c_\nu^2 \\ d_\nu^2 \end{bmatrix} = -\left[Q^2\right]^{-1} \begin{bmatrix} a_q^2 \\ b_q^2 \end{bmatrix} + \left[T^{21}\right] \begin{bmatrix} c_\nu^1 \\ d_\nu^1 \end{bmatrix} \tag{4.52}$$

where

$$\left[T^{21}\right] = -\left[Q^2\right]^{-1} \left[Q^{21}\right]. \tag{4.53}$$

Using Eqs. (4.50) and (4.52) field on the surface of the scatterers is found as

$$\begin{bmatrix} c_\nu^1 \\ d_\nu^1 \end{bmatrix} = -\left\{\left[I\right] - \left[T^{12}\right]\left[T^{21}\right]\right\}^{-1} \left\{\left[Q^1\right]^{-1} \begin{bmatrix} a_q^1 \\ b_q^1 \end{bmatrix} + \left[T^{12}\right]\left[Q^2\right]^{-1} \begin{bmatrix} a_q^2 \\ b_q^2 \end{bmatrix}\right\} \tag{4.54}$$

and

$$\begin{bmatrix} c_\nu^2 \\ d_\nu^2 \end{bmatrix} = -\left\{\left[I\right] - \left[T^{21}\right]\left[T^{12}\right]\right\}^{-1} \left\{\left[Q^2\right]^{-1} \begin{bmatrix} a_q^2 \\ b_q^2 \end{bmatrix} + \left[T^{21}\right]\left[Q^1\right]^{-1} \begin{bmatrix} a_q^1 \\ b_q^1 \end{bmatrix}\right\} \tag{4.55}$$

where $[I]$ is the identity matrix.

Scattered field from each object can be expanded as

$$\bar{E}_1^s(\bar{R}_1) = \sum_p R_p[e_p^1 \bar{M}_{ep}^{(4)}(k_0 \bar{R}_1) + f_p^1 \bar{N}_{op}^{(4)}(k_0 \bar{R}_1)] \tag{4.56}$$

$$\bar{E}_2^s(\bar{R}_2) = \sum_p R_p[e_p^2 \bar{M}_{ep}^{(4)}(k_0 \bar{R}_2) + f_p^2 \bar{N}_{op}^{(4)}(k_0 \bar{R}_2)] \tag{4.57}$$

where $\bar{E}_1^s$ and $\bar{E}_2^s$ are the scattered field form object 1 and object 2, respectively. Unknown coefficients can be determined based on c_ν and d_ν by applying the Green's second identity over the circumscribing spheres. Resulting matrix relations are

$$\begin{bmatrix} e_p^1 \\ f_p^1 \end{bmatrix} = \underbrace{\begin{bmatrix} J_{p\nu}^{1'} & I_{p\nu}^{1'} \\ L_{p\nu}^{1'} & K_{p\nu}^{1'} \end{bmatrix}}_{[Q_e^1]} \begin{bmatrix} c_\nu^1 \\ d_\nu^1 \end{bmatrix} \tag{4.58}$$

$$\begin{bmatrix} e_p^2 \\ f_p^2 \end{bmatrix} = \underbrace{\begin{bmatrix} J_{p\nu}^{2'} & I_{p\nu}^{2'} \\ L_{p\nu}^{2'} & K_{p\nu}^{2'} \end{bmatrix}}_{[Q_e^2]} \begin{bmatrix} c_\nu^2 \\ d_\nu^2 \end{bmatrix} \tag{4.59}$$

Elements of the $[Q_e^k]$ matrix is defined as

$$J_{p\nu}^{k'} = \int\limits_{S_{S_k}} [\bar{M}_{e\nu}^{(1)}(k_0\bar{R}_k') \times \bar{A}_p^{k(1)}] \centerdot \hat{n}_k' \mathrm{d}s' \tag{4.60}$$

$$I_{p\nu}^{k'} = \int\limits_{S_{S_k}} [\bar{N}_{o\nu}^{(1)}(k_0\bar{R}_k') \times \bar{A}_p^{k(1)}] \centerdot \hat{n}_k' \mathrm{d}s' \tag{4.61}$$

$$L_{p\nu}^{k'} = \int\limits_{S_{S_k}} [\bar{M}_{e\nu}^{(1)}(k_0\bar{R}_k') \times \bar{B}_p^{k(1)}] \centerdot \hat{n}_k' \mathrm{d}s' \tag{4.62}$$

$$K_{p\nu}^{k'} = \int\limits_{S_{S_k}} [\bar{N}_{o\nu}^{(1)}(k_0\bar{R}_k') \times \bar{B}_p^{k(1)}] \centerdot \hat{n}_k' \mathrm{d}s' \tag{4.63}$$

where k represents the scatterer 1 or scatterer 2 and

$$\bar{A}_p^{k(1)} = \frac{jk_0Z_0}{\eta_k}[\hat{n}_k' \times \bar{M}_{ep}^{(1)}(k_0\bar{R}_k')] - k_0\bar{N}_{ep}^{(1)}(k_0\bar{R}_k') \tag{4.64}$$

$$\bar{B}_p^{k(1)} = \frac{jk_0Z_0}{\eta_k}[\hat{n}_k' \times \bar{N}_{op}^{(1)}(k_0\bar{R}_k')] - k_0\bar{M}_{op}^{(1)}(k_0\bar{R}_k') \tag{4.65}$$

Upon substitution of Eqs. (4.54) and (4.55) in Eqs. (4.58) and (4.59), respectively, coefficients of the scattered field by each object can be calculated. Total field is the sum of theses two fields,

$$\bar{E}^s(\bar{R}) = \bar{E}_1^s(\bar{R}_1) + \bar{E}_2^s(\bar{R}_2). \tag{4.66}$$

4.2 Numerical Results

In this section we use the T-matrix formulation for the two identical spherical scatterers at the edge of a half-plane. Geometry of the problem is illustrated in Fig. 4.2. The radius of scatterers are assumed as $\lambda/4$ and their surface impedance is assigned as $\eta_{1,2} = 1.5Z_0$. Spheres are separated by a distance of 3λ.

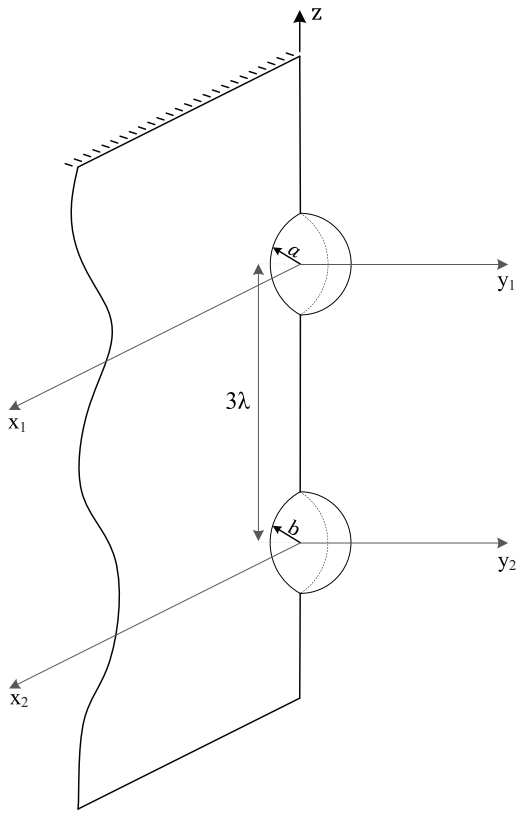

Figure 4.2: Two spherical scatterers at the edge of a half-plane

In Figs. 4.3 – 4.9, far zone mono-static scattering patterns are plotted for $\theta_0 = 1°, 10°, 20°, 40°, 60°$ and $80°$. In the far-field calculations, unit vectors of the two coordinates in the $\hat{\theta}$ direction are assumed to be parallel. For the amplitude, radial distance is approximated as $|\bar{R}_1| = |\bar{R}_2| = R$ and for the phase, $-k_0 d\cos(\theta_0)$ phase difference is assumed.

It is observed that in the paraxial region, due to the edge excited waves the scattering field intensity is higher. In addition, field intensity varies as $\sin^2(\frac{\phi}{2})$

and $\cos^2(\frac{\phi}{2})$ for $\theta\theta$ and $\phi\phi$ polarizations, respectively, which indicates that the $m = 0, n = 1$ mode is dominant. Away from paraxial region, effect of edge guided waves decreases therefore mutual interference between object becomes significant.

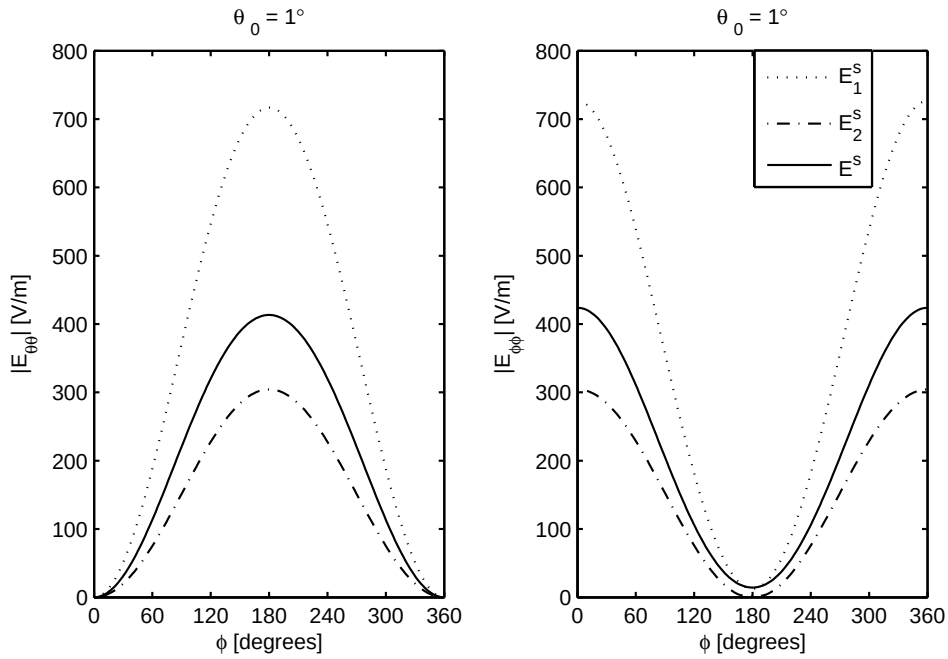

Figure 4.3: Monostatic scattered field pattern for $a = b = 0.25\lambda$, $\eta_1 = \eta_2 = 1.5Z_0$, $\gamma = 2\pi$, $d = 3\lambda$ and $\theta_0 = 1°$.

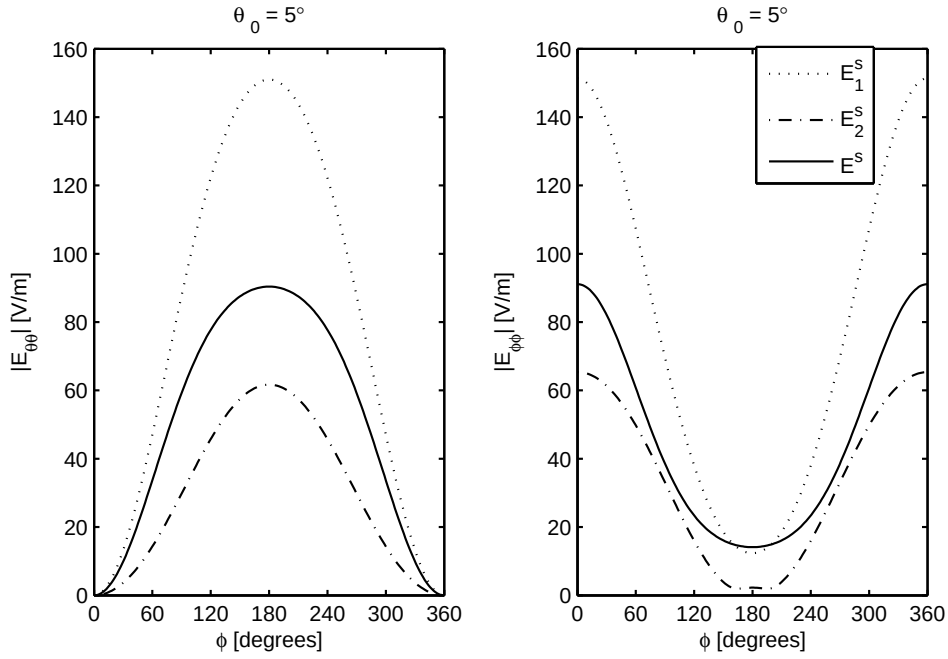

Figure 4.4: Monostatic scattered field pattern for $a = b = 0.25\lambda$, $\eta_1 = \eta_2 = 1.5Z_0$, $\gamma = 2\pi$, $d = 3\lambda$ and $\theta_0 = 5°$.

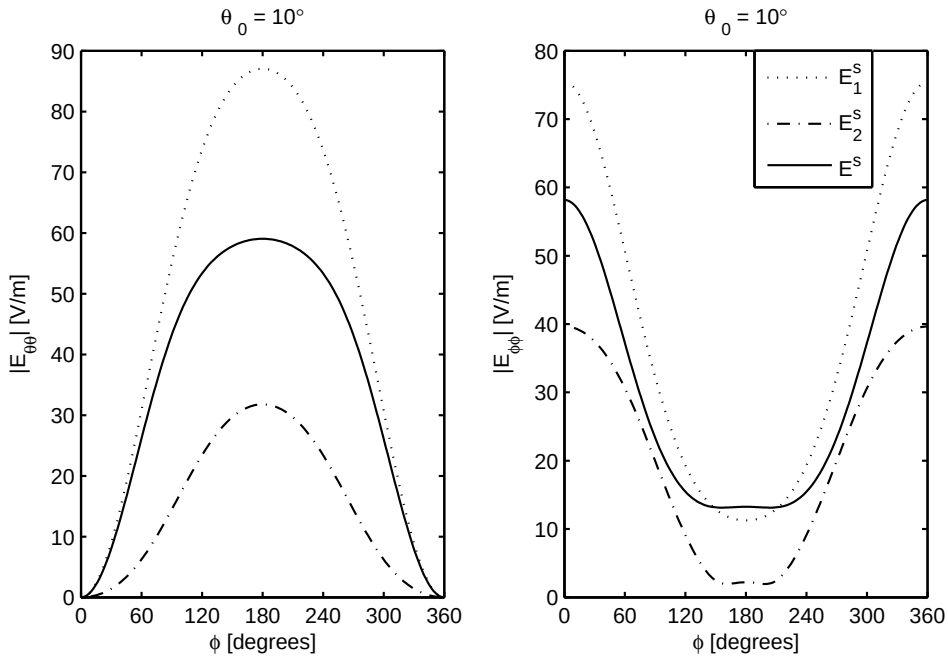

Figure 4.5: Monostatic scattered field pattern for $a = b = 0.25\lambda$, $\eta_1 = \eta_2 = 1.5Z_0$, $\gamma = 2\pi$, $d = 3\lambda$ and $\theta_0 = 10°$.

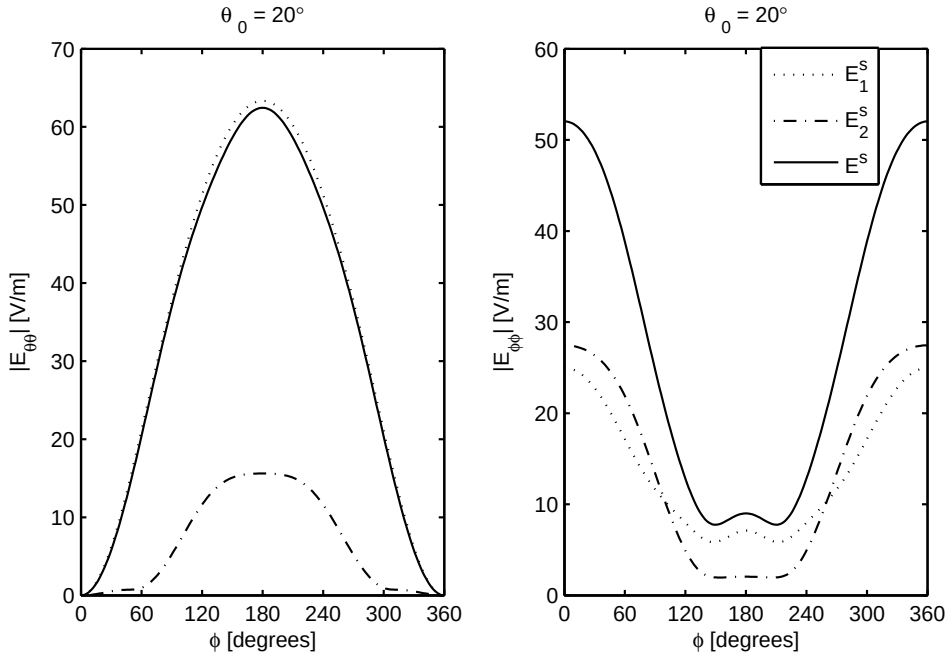

Figure 4.6: Monostatic scattered field pattern for $a = b = 0.25\lambda$, $\eta_1 = \eta_2 = 1.5Z_0$, $\gamma = 2\pi$, $d = 3\lambda$ and $\theta_0 = 20°$.

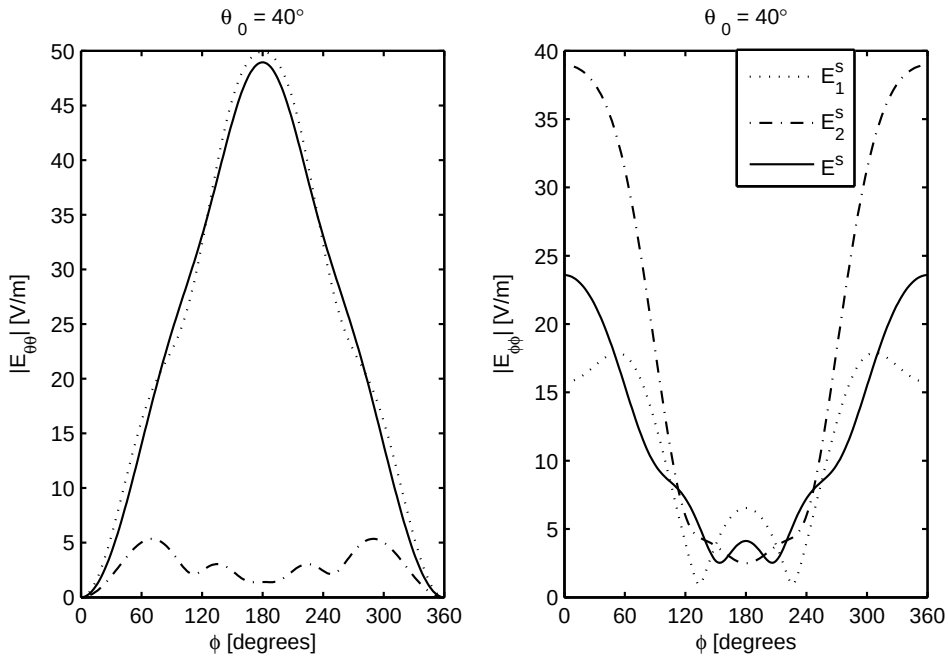

Figure 4.7: Monostatic scattered field pattern for $a = b = 0.25\lambda$, $\gamma = 2\pi$, $\eta_1 = \eta_2 = 1.5Z_0$, $d = 3\lambda$ and $\theta_0 = 40°$.

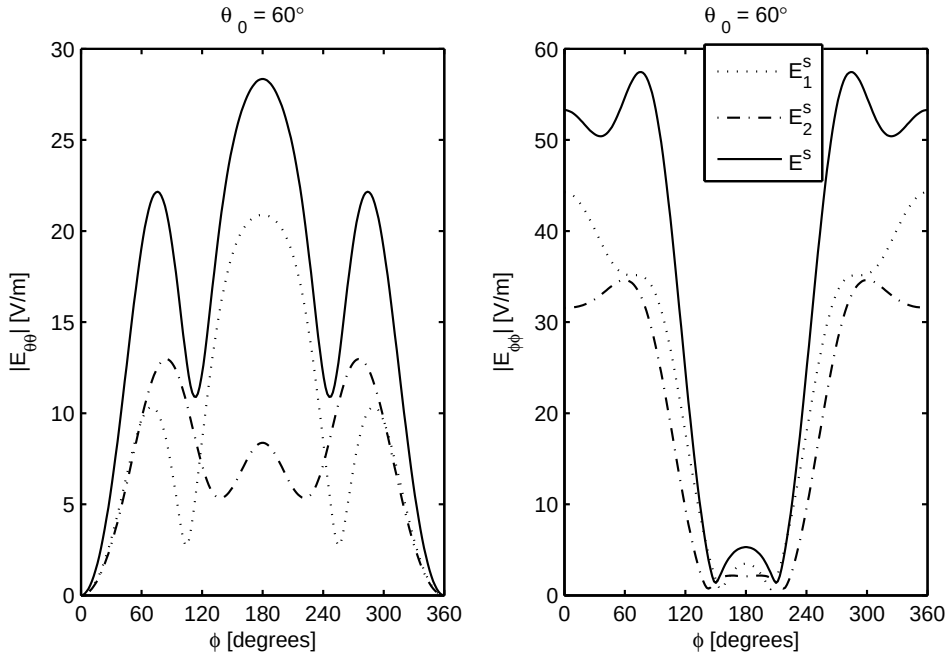

Figure 4.8: Monostatic scattered field pattern for $a = b = 0.25\lambda$, $\eta_1 = \eta_2 = 1.5Z_0$, $\gamma = 2\pi$, $d = 3\lambda$ and $\theta_0 = 60°$.

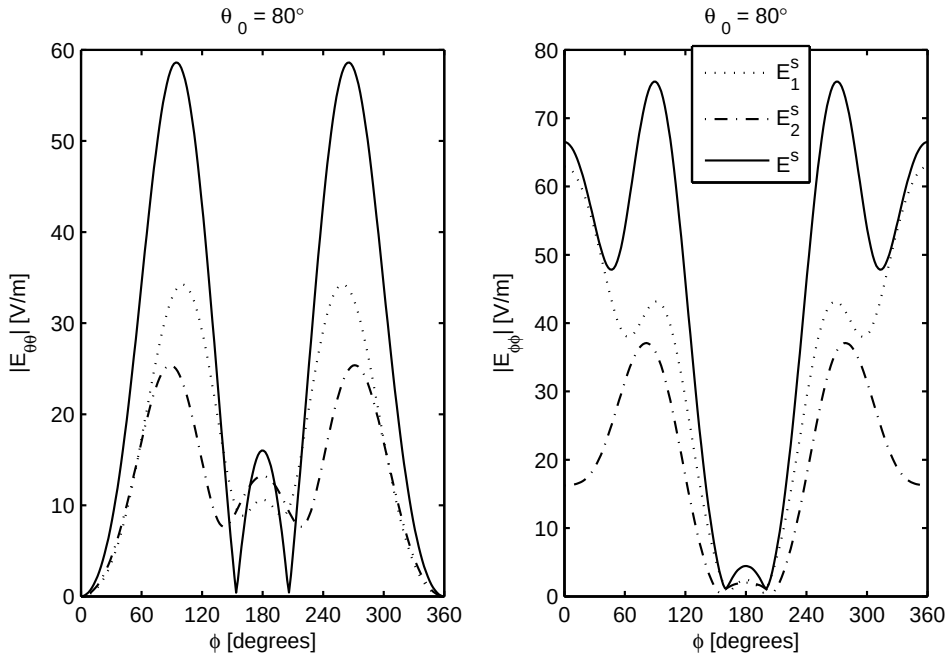

Figure 4.9: Monostatic scattered field pattern for $a = b = 0.25\lambda$, $\gamma = 2\pi$, $d = 3\lambda$ and $\theta_0 = 80°$.

limiting case of PEC scatterers (i.e. $\eta \to 0$), is investigated by assigning $\eta = 10^{-12}$ and the results are compared with the one obtained from the formulation given in [7]. Figs. 4.10 – 4.15 show the monostatic scattered field for two PEC scatterer of radius $\lambda/4$ separated by a distance of 3λ. Results obtained from two formulations are in perfect agreement.

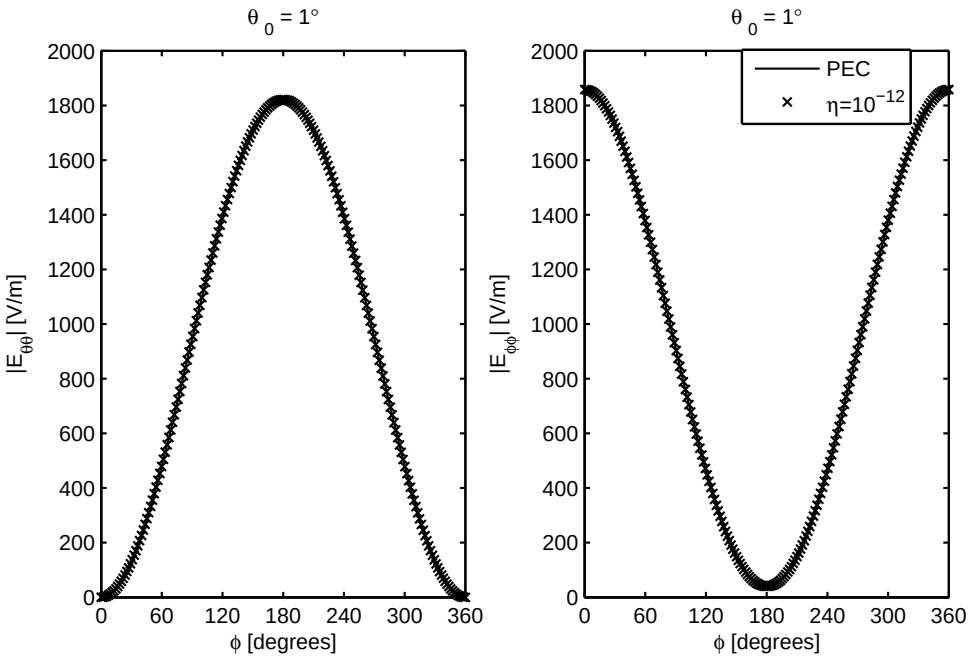

Figure 4.10: Monostatic scattered field pattern for PEC case, $a = b = 0.25\lambda$, $\gamma = 2\pi$, $d = 3\lambda$ and $\theta_0 = 1°$.

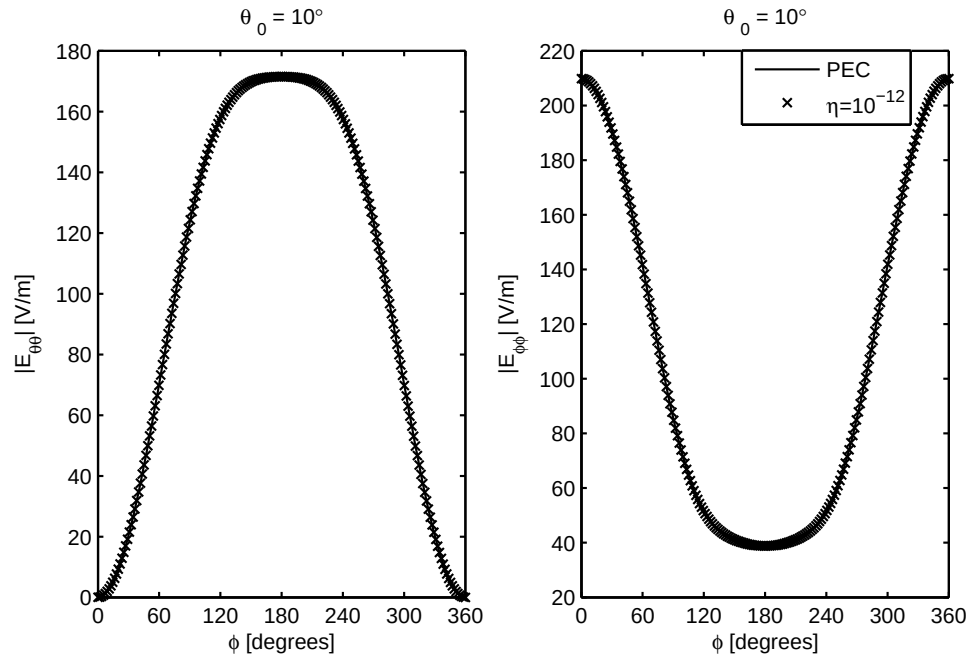

Figure 4.11: Monostatic scattered field pattern for PEC case, $a = b = 0.25\lambda$, $\gamma = 2\pi$, $d = 3\lambda$ and $\theta_0 = 10°$.

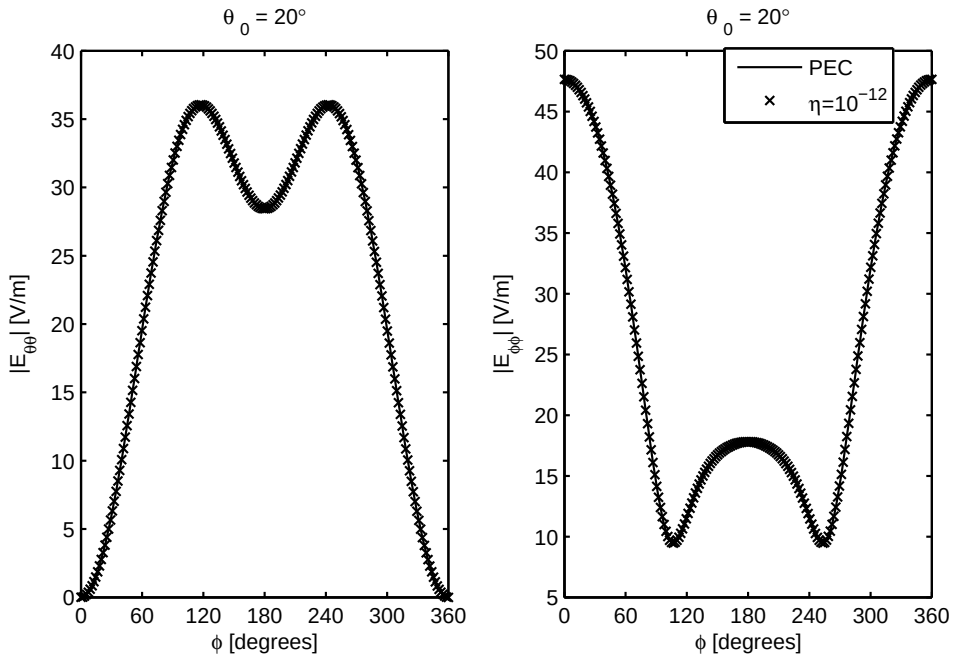

Figure 4.12: Monostatic scattered field pattern for PEC case, $a = b = 0.25\lambda$, $\gamma = 2\pi$, $d = 3\lambda$ and $\theta_0 = 20°$.

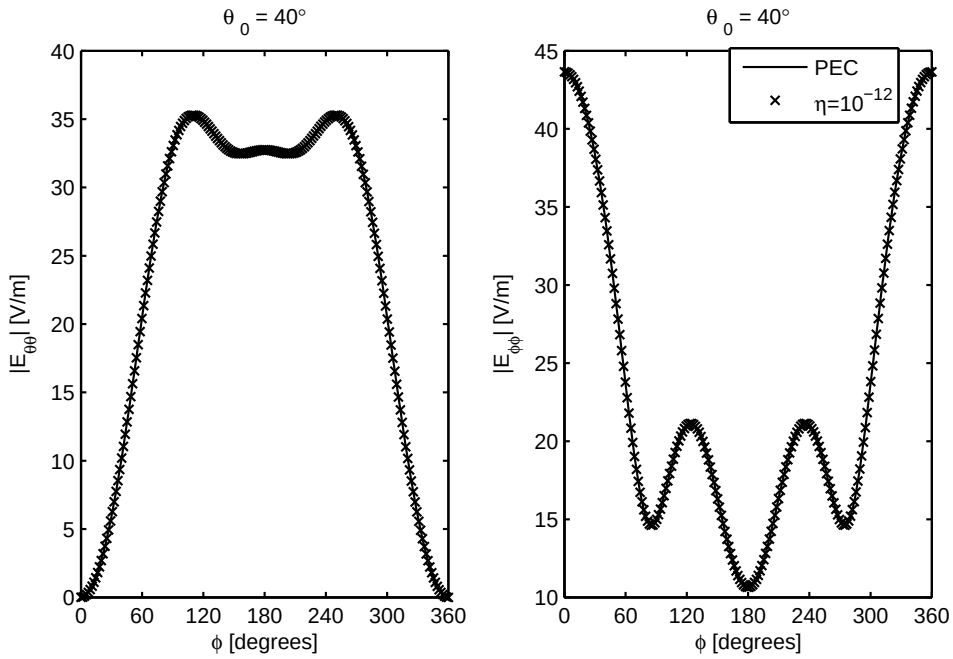

Figure 4.13: Monostatic scattered field pattern for PEC case, $a = b = 0.25\lambda$, $\gamma = 2\pi$, $d = 3\lambda$ and $\theta_0 = 40°$.

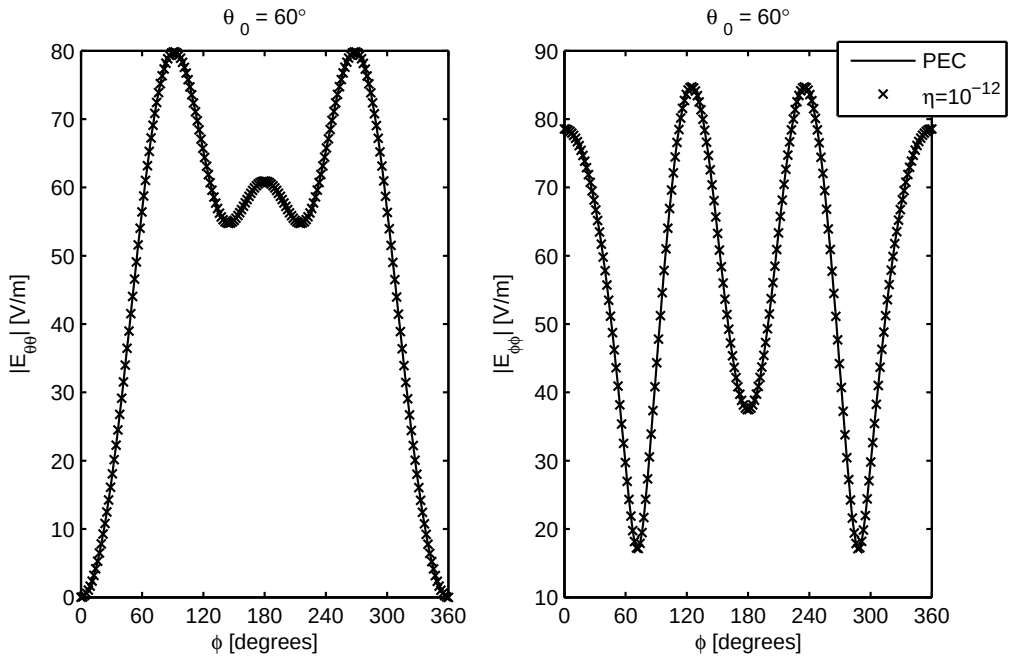

Figure 4.14: Monostatic scattered field pattern for PEC case, $a = b = 0.25\lambda$, $\gamma = 2\pi$, $d = 3\lambda$ and $\theta_0 = 60°$.

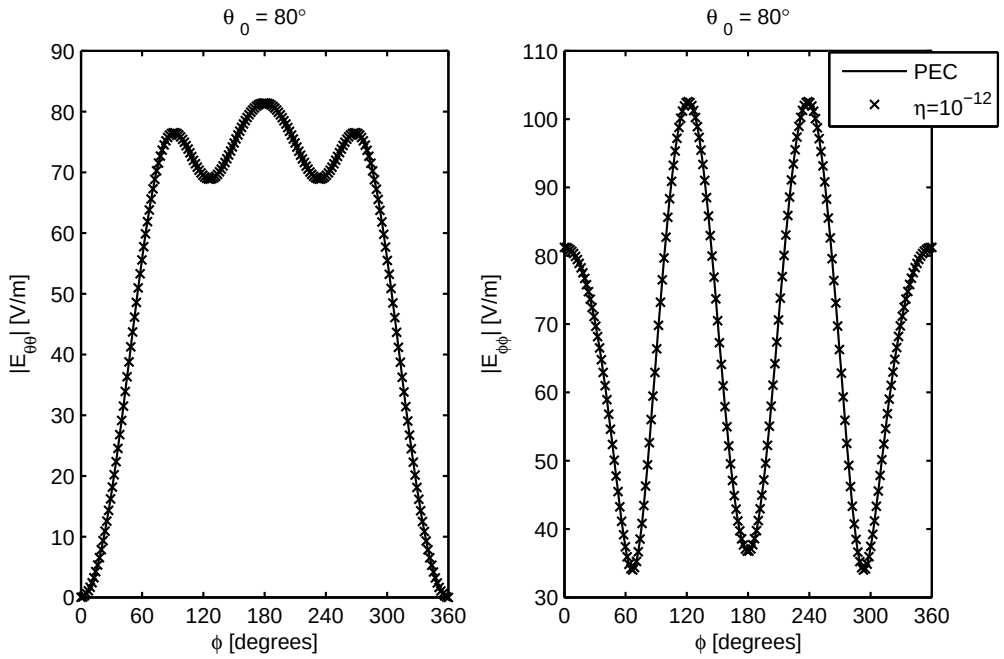

Figure 4.15: Monostatic scattered field pattern for PEC case, $a = b = 0.25\lambda$, $\gamma = 2\pi$, $d = 3\lambda$ and $\theta_0 = 80°$.

4.3 Multiple Scatterers

For more than two scatterers at the edge, described T-matrix formulation can be generalized by taking the similar steps. For N scatterers, N coordinates systems are defined that their origins are denoted as $O_1, O_2, O_3, \ldots O_N$. Position vector in kth coordinates is denoted as $\bar{R}_k$. Incident field, the field in the presence of the wedge, in kth coordinates is defined as,

$$\bar{E}^0 = \sum_q R_q \left[a_q^k \bar{M}_{eq}^{(1)}(k_0 \bar{R}_k) + b_q^k \bar{N}_{oq}^{(1)}(k_0 \bar{R}_k) \right], \quad k = 1, 2, \ldots, N \tag{4.67}$$

where a_q^k and b_q^k are known. Total incident field on kth scatterer is the sum of $\bar{E}^0$ and the scattered field from other objects.

$$\bar{E}_k^i(\bar{R}_k) = \sum_q R_q \left[(a_q^k + \sum_{\substack{j=1 \\ j \neq k}}^{N} g^{kj}) \bar{M}_{eq}^{(1)}(k_0 \bar{R}_k) + (b_q^k + \sum_{\substack{j=1 \\ j \neq k}}^{N} h^{kj}) \bar{N}_{oq}^{(1)}(k_0 \bar{R}_k) \right], \quad k = 1, 2, \ldots, N \tag{4.68}$$

where g^{kj} and h^{kj} are the coefficients of the scattered field form jth object incident on kth scatterer. These coefficients are yet to be determined. Electric field on the surface of each scatterer can be expanded as

$$\bar{E}(\bar{R}_k) = \sum_\nu c_\nu^k \bar{M}_{e\nu}^{(1)}(k_0 \bar{R}_k) + d_\nu^k \bar{N}_{o\nu}^{(1)}(k_0 \bar{R}_k) \tag{4.69}$$

each set of unknowns for each scatterer can be found similarly to Eq. (4.50) as

$$\begin{bmatrix} c_\nu^k \\ d_\nu^k \end{bmatrix} = - \left[Q^k \right]^{-1} \begin{bmatrix} a_q^k \\ b_q^k \end{bmatrix} + \sum_{\substack{j=1 \\ j \neq k}}^{N} \left[T^{kj} \right] \begin{bmatrix} c_\nu^j \\ d_\nu^j \end{bmatrix}, \quad k = 1, 2, \ldots N \tag{4.70}$$

where $[Q^k]$ is the Q-matrix for kth scatterer and $[T^{kj}]$ represents the incident field on kth body due to the scattering from jth body.

$$\left[T^{kj} \right] = - \left[Q^k \right]^{-1} \left[Q^{kj} \right] \tag{4.71}$$

Q^{kj} is partitioned as follows

$$\left[Q^{kj} \right] = \begin{bmatrix} J_{q\nu}^{kj} & I_{q\nu}^{kj} \\ L_{q\nu}^{kj} & K_{q\nu}^{kj} \end{bmatrix} \tag{4.72}$$

where

$$J_{q\nu}^{kj} = \int_{S_j} \left[\bar{M}_{e\nu}^{(1)}(k_0\bar{R}_j') \times \bar{G}_q^{kj}\right] \cdot \hat{n}_j \mathrm{d}s' \tag{4.73}$$

$$I_{q\nu}^{kj} = \int_{S_j} \left[\bar{N}_{o\nu}^{(1)}(k_0\bar{R}_j') \times \bar{G}_q^{kj}\right] \cdot \hat{n}_j \mathrm{d}s' \tag{4.74}$$

$$L_{q\nu}^{kj} = \int_{S_j} \left[\bar{M}_{e\nu}^{(1)}(k_0\bar{R}_j') \times \bar{H}_q^{kj}\right] \cdot \hat{n}_j \mathrm{d}s' \tag{4.75}$$

$$K_{q\nu}^{kj} = \int_{S_j} \left[\bar{N}_{o\nu}^{(1)}(k_0\bar{R}_j') \times \bar{H}_q^{kj}\right] \cdot \hat{n}_j \mathrm{d}s' \tag{4.76}$$

with

$$\bar{G}_q^{kj} = \frac{jk_0Z_0}{\eta_j}[\hat{n}_j' \times \bar{M}_{eq}^{(4)}(k_0\bar{R}_k')] - \nabla_j \times \bar{M}_{eq}^{(4)}(k_0\bar{R}_k') \tag{4.77}$$

$$\bar{H}_q^{kj} = \frac{jk_0Z_0}{\eta_j}[\hat{n}_j' \times \bar{N}_{oq}^{(4)}(k_0\bar{R}_k')] - \nabla_j \times \bar{N}_{oq}^{(4)}(k_0\bar{R}_k') \tag{4.78}$$

S_j and $\hat{n}_j$ denote surface of the jth scatterer and its unit vector, respectively. $\nabla_j\times$ represents the curl operation in the kth coordinates.

Scattered field from each scatterer can be found once the unknown coefficients c_ν^k and d_ν^k are calculated. Scattered field coefficients of the kth scatterer is defined as,

$$\begin{bmatrix} e_p^k \\ f_p^k \end{bmatrix} = \left[Q_e^k\right] \begin{bmatrix} c_\nu^k \\ d_\nu^k \end{bmatrix} \tag{4.79}$$

where $[Q_e^k]$ is defined in Eqs. (4.60) to (4.63). Scattered field from each scatterer is given by

$$\bar{E}_k^s(\bar{R}_k) = \sum_p [e_p^k \bar{M}_{ep}^{(4)}(k_0\bar{R}_k) + f_p^k \bar{N}_{op}^{(4)}(k_0\bar{R}_k)], \quad k = 1, 2, \ldots N \tag{4.80}$$

Total field is the sum of the scattered field from each scatterer

$$\bar{E}^s(\bar{R}) = \sum_{k=1}^{N} \bar{E}_k^s(\bar{R}_k) \tag{4.81}$$

Chapter 5

Conclusion

In this thesis, scattering from impedance bodies positioned at the edge of a PEC wedge is studied. The problem is treated by employing the eigenfunction expansion technique.

For the simple case of a spherical boss at the edge, complete dyadic Green's function has been obtained which is valid everywhere in space and it includes the singular term which is valid in the source region. We showed that the Green's function can be decomposed into two parts. One part is the dyadic Green's function of the wedge with scatterer removed and the other part includes the contribution of the boss and the mutual interaction of the scatterer and the wedge. Analytically it was shown that in the limiting case of PEC scatterer, the expressions reduces to the solution given in [7]. Numerical examples are presented and we observed that the scattering is enhanced in the paraxial region due to the edge excited waves. We found that first term in the eigenfunction expansion is dominant in the paraxial region. As we move away from the edge higher order modes are excited. An investigation of convergence of the series was also presented in Chapter 2 showing that truncation size increases as the boss radius and the exterior wedge angle increase.

In Chapter 3, T-matrix formulation was introduced which extends the Green's function solution for irregularly shaped impedance scatterer. The solution has

verified analytically by applying for spherical scatterer at the origin. In order to simulate an irregularly shaped object, a sphere positioned off the origin is considered and scattered field is calculated and compared with the exact solution. Excellent agreement is achieved between two solutions. Accuracy and convergence of the T-matrix solution depends on the geometry of the scatterer. For large scatterers and cases for which center of symmetry is considered away from the origin, higher order terms are needed and resulting T-matrix is ill-conditioned. Therefore, accurate results cannot be achieved.

In Chapter 4, a complete modal solution using T-matrix method is developed for multiple scatterers at the edge which includes mutual influence of the scatterers. First, formulation is developed for two impedance bodies and numerical results are provided. It is observed that, near grazing incidence, scattering due to the edge excited wave is dominant. However, as we move away from the edge, mutual interference between scatterers becomes dominant. Finally, the solution is generalized for the case of more than two scatterers.

Future work may include asymptotic solution of the proposed eigenfunction expansion in order to extend the current high-frequency approaches for scattering from objects at the edge. In this manner, simple expressions should be obtained for the scattered field from impedance bodies at the edge. Since contribution of scatterer and the wedge is separated, these expression can be integrated into current high-frequency solutions for the wedge.

Bibliography

[1] J. B. Keller, "How dark is the shadow of a round-ended screen?," *J. Appl. Phys.*, vol. 30, no. 9, pp. 1452–1454, 1959.

[2] R. Kouyoumjian and W. D. Bourside, "The diffraction by a cylinder-tipped half-plane," *IEEE Trans. Antennas Propag.*, vol. 18, pp. 424–426, May 1970.

[3] W. Hallidy, "On uniform asymptotic green's functions for the perfectly conducting cylinder tipped wedge," *IEEE Trans. Antennas Propag.*, vol. AP-33, pp. 1020–1025, Sept. 1985.

[4] A. C. Polycarpou and M. A. Christou, "Full-wave scattering from a grooved cylinder-tipped conducting wedge," *IEEE Trans. Antennas Propag.*, vol. 59, pp. 2732–2735, July 2011.

[5] A. Borgioli, R. Coccioli, G. Pelosi, and J. L. Volakis, "Electromagnetic scattering from a corrugated wedge," *IEEE Trans. Antennas Propag.*, vol. 45, pp. 1265–1268, Aug. 1997.

[6] G. Pelosi, R. Coccioli, G. Manara, and A. Monorchio, "Scattering from a wedge with cavity backed apertures in its faces and related configurations: Te case," *IEE Proc.-Microw. Antennas Propag.*, vol. 142, pp. 183–188, Apr. 1995.

[7] O. M. Buyukdura, *Radiation from Sources and Scatterers near the Edge of a Perfectly Conducting Wedge.* PhD thesis, The Ohio State University, 1984.

[8] P. H. Pathak, "On the eigenfunction expansion of electromagnetic dyadic green's functions," *IEEE Trans. Antennas Propag.*, vol. AP-31, pp. 837–846, Nov. 1983.

[9] J. L. Volakis and T. B. A. Senior, *Approximate boundary conditions in electromagnetics*. London, United Kingdom: The Institution of Electrical Engineers, 1995.

[10] J. Meixner, "The behavior of electromagnetic fields at edges," *IEEE Trans. Antennas Propag.*, vol. AP-20, pp. 442–446, July 1972.

[11] P. M. Morse and H. Feshbach, *Methods of Theoretical Physics*. McGraw-Hill Book Company, Inc., 1953.

[12] O. M. Buyukdura, S. D. Goad, and R. G. Kouyoumjian, "A spherical wave representation of the dyadic green's function for a wedge," *IEEE Trans. Antennas Propag.*, vol. 44, pp. 12–22, Jan. 1996.

[13] M. Abramowitz and I. A. Stegun, *Handbook of Mathematical Functions with Formulas, Graphs, and Mathematical Tables*. New York: Dover, 1964.

[14] C. T. Tai, "Equivalent layers of surface charge, current sheet, and polarization in the eigenfunction expansion of green's functions in electromagnetic theory," *IEEE Trans. Antennas Propag.*, vol. AP-29, pp. 733–739, Sept. 1981.

[15] P. C. Waterman, "Matrix formulation of electromagnetic scattering," *Proceedings of the IEEE*, vol. 53, pp. 805–810, Aug. 1965.

[16] P. C. Waterman, "Symmetry, unitarity, and geometry in electromagnetic scattering," *Physical review D*, vol. 3, pp. 825–839, Feb. 1971.

[17] V. K. Varadan and V. V. Varadan, eds., *Acoustic, Electromagnetic and Elastic Wave Scattering: Focus on the T-matrix Approach - International Symposium held at The Ohio State University, Columbus, Ohio, USA, June 25-27, 1979*. Pergamon Press, 1980.

[18] C.-T. Tai, *Dyadic Green's Functions in Electromagnetic Theory*. Intext Educational Publishers, 1971.

Appendix A

Spherical Vector Wave Functions

In this Appendix, spherical vector wave function will be introduced and orthogonality relations are presented. First scalar wave functions are defined, then the vector wave functions are introduced according to the scalar functions. Finally, the orthogonality relationship of these functions are given. Detailed study of vector wave functions are given in [11], [18] and [12], here the summary of these works are presented.

A.1 Spherical Scalar Wave Functions

Scalar wave functions are the solution of the scalar wave equation given as

$$(\nabla^2 + k^2)\psi(\bar{R}) = 0. \tag{A.1}$$

Solution of Eq. (A.1) in the spherical coordinates can be found using separation of variables techniques as

$$\psi(\bar{R}) = R(r)\Theta(\theta)\Phi(\phi) \tag{A.2}$$

where

$$R(r) = \begin{cases} j_\nu(kr) \\ h_\nu^{(2)}(kr) \end{cases} \tag{A.3}$$

$$\Theta(\theta) = \begin{cases} P_\nu^{-\mu}(\cos\theta) \\ Q_\nu^{-\mu}(\cos\theta) \end{cases} \tag{A.4}$$

$$\Phi(\phi) = \begin{cases} \cos(\mu\phi) \\ \sin(\mu\phi) \end{cases} \tag{A.5}$$

where μ and ν are the separation variables which will be defined based on the boundary conditions.

In Eq. (A.3), $j_\nu(kr)$ is the spherical Bessel function which is regular at the origin and $h_\nu^{(2)}(kr)$ is the spherical Hankel function which satisfies the radiation condition as $r \to \infty$ for the $e^{j\omega t}$ time dependence. In the development of the dyadic Green's function combination of these two functions are used and is represented as

$$R(r) = z_\nu^{(t)}(kr) = Aj_\nu(kr) + Bh_\nu^{(2)}(kr) \tag{A.6}$$

where A and B are constants to be defined by the boundary conditions and superscript (t) identifies the type of the combination used. For the cases where one of the constants is zero

$$z_\nu^{(1)}(kr) = j_\nu(kr) \tag{A.7}$$

$$z_\nu^{(4)}(kr) = h_\nu^{(2)}(kr). \tag{A.8}$$

In Eq. (A.4), $P_\nu^{-\mu}(\cos\theta)$ and $Q_\nu^{-\mu}(\cos\theta)$ are the associated Legendre functions of the first and second kind, respectively. It will be seen that Dyadic Green's function should satisfy the edge condition hence it should be bounded at $\theta = 0, \pi$, consequently, associated Legendre functions of the second kind should be excluded from the solution because it is not bounded at these points. Also, associated Legendre function of the first kind is slightly modified and Ferrer's type Legendre functions are used for convenience [12]. This function is related to the associated Legendre of first kind by a complex constant and it is denoted by T.

$$\Theta(\theta) = T_\nu^{-\mu}(\cos\theta) \tag{A.9}$$

It is shown in [12] that in order to avoid the singularities within the interval of $[0, \pi]$, sum of the degree, ν, and order, $-\mu$ should be an integer. It is critical

because the scalar functions must satisfy the edge condition. To satisfy this condition, let

$$\nu = n + \mu \tag{A.10}$$

where n is an integer. Completeness and orthogonality of Ferrer's type Legendre functions and also useful information for calculating these functions are presented in [12].

The scalar wave functions can now be introduced using Eqs. (A.2) and (A.6) – (A.10) as

$$\psi^{(t)}_{\substack{e\\o}\mu n}(k\bar{R}) = z^{(t)}_{\mu+n}(kr)\, T^{-\mu}_{\mu+n}(\cos\theta) \begin{matrix}\cos\\ \sin\end{matrix}(\mu\phi) \tag{A.11}$$

where e and o represents even and odd functions respectively.

A.2 Spherical Vector Wave Functions

In this section vector wave functions will be constructed based on the scalar wave functions. Solenoidal vector wave functions satisfies the homogeneous vector wave equation,

$$\nabla \times \nabla \times \bar{F} - k^2 \bar{F} = 0. \tag{A.12}$$

It is shown in [11] and [18] that two sets of solutions based on the spherical scalar wave functions can be obtained. They are

$$\bar{M}^{(t)}_{\substack{e\\o}\mu n}(k\bar{R}) = \nabla \times [k\bar{R}\, \psi^{(t)}_{\substack{e\\o}\mu n}(k\bar{R})] \tag{A.13}$$

and

$$\bar{N}^{(t)}_{\substack{e\\o}\mu n}(k\bar{R}) = \nabla \times \nabla \times [\bar{R}\, \psi^{(t)}_{\substack{e\\o}\mu n}(k\bar{R})] \tag{A.14}$$

This vector wave functions are solenoidal so they satisfy

$$\nabla \cdot \begin{bmatrix} \bar{M}^{(t)}_{\substack{e\\o}\mu n}(k\bar{R}) \\ \bar{N}^{(t)}_{\substack{e\\o}\mu n}(k\bar{R}) \end{bmatrix} = 0 \tag{A.15}$$

and they have the following symmetry relations

$$\bar{M}_q = \frac{1}{k} \nabla \times \bar{N}_q \tag{A.16}$$

$$\bar{N}_q = \frac{1}{k}\nabla \times \bar{M}_q \tag{A.17}$$

where q represents the collection ${}^{e}_{o}\mu n$.

Performing the differential operations in Eqs. (A.13) and (A.14), vector wave functions can be explicitly shown as

$$\bar{M}^{(t)}_{{}^{e}_{o}\mu n}(k\bar{R}) = kz^{(t)}_{\mu+n}(kr)\bar{m}_{{}^{e}_{o}\mu n}(\theta,\phi), \tag{A.18}$$

$$\bar{N}^{(t)}_{{}^{e}_{o}\mu n}(k\bar{R}) = \frac{1}{r}z^{(t)}_{\mu+n}(kr)\bar{l}_{{}^{e}_{o}\mu n}(\theta,\phi) + \frac{1}{r}\frac{d}{dr}[rz^{(t)}_{\mu+n}(kr)]\bar{n}_{{}^{e}_{o}\mu n}(\theta,\phi) \tag{A.19}$$

where $\bar{m}_{{}^{e}_{o}\mu n}(\theta,\phi)$, $\bar{n}_{{}^{e}_{o}\mu n}(\theta,\phi)$ and $\bar{l}_{{}^{e}_{o}\mu n}(\theta,\phi)$ are the auxiliary vector wave function. They are simply defined by factoring out the radial dependence.

$$\bar{m}_{{}^{e}_{o}\mu n}(\theta,\phi) = \frac{\mp\mu \begin{matrix}\sin\\ \cos\end{matrix}(\mu\phi)T^{-\mu}_{\mu+n}(\cos\theta)}{\sin\theta}\,\hat{\theta} - \begin{matrix}\cos\\ \sin\end{matrix}(\mu\phi)\frac{d}{d\theta}[T^{-\mu}_{\mu+n}(\cos\theta)]\,\hat{\phi} \tag{A.20}$$

$$\bar{n}_{{}^{e}_{o}\mu n}(\theta,\phi) = \hat{r}\times\bar{m}_{{}^{e}_{o}\mu n}(\theta,\phi) \tag{A.21}$$

$$= \begin{matrix}\cos\\ \sin\end{matrix}(\mu\phi)\frac{d}{d\theta}[T^{-\mu}_{\mu+n}(\cos\theta)]\,\hat{\theta} \mp \frac{\mu \begin{matrix}\sin\\ \cos\end{matrix}(\mu\phi)T^{-\mu}_{\mu+n}(\cos\theta)}{\sin\theta}\,\hat{\phi} \tag{A.22}$$

$$\bar{l}_{{}^{e}_{o}\mu n}(\theta,\phi) = (\mu+n)(\mu+n+1)\begin{matrix}\cos\\ \sin\end{matrix}(\mu\phi)T^{-\mu}_{\mu+n}(\cos\theta)\,\hat{r} \tag{A.23}$$

$\hat{r},\hat{\theta},\hat{\phi}$ represents the unit vectors in the spherical coordinates.

Here, the irrotational vector wave function is not presented since they will not be used in the solution of the problem addressed in this study.

In [12], orthogonality and completeness of the auxiliary vector wave functions over a spherical surface exterior to wedge are examined. In the following orthogonality relations surface integration is defined as

$$\int_{\Omega_0}(\,\blacksquare\,)\mathrm{d}\,\Omega = \int_{\phi=0}^{\gamma}\int_{\theta=0}^{\pi}(\,\blacksquare\,)\sin\theta\,\mathrm{d}\theta\,\mathrm{d}\phi \tag{A.24}$$

Orthogonality relations are as follows

$$\int_{\Omega_0} \bar{m}_q(\theta,\phi) \cdot \bar{m}_{q'}(\theta,\phi)\,\mathrm{d}\Omega = \frac{\epsilon_m \gamma n!(\mu+n)(\mu+n+1)}{(2\mu+2n+1)\Gamma(2\mu+n+1)}\delta_{\mu\mu'}\delta_{nn'} \tag{A.25}$$

$$\int_{\Omega_0} \bar{n}_q(\theta,\phi) \cdot \bar{n}_{q'}(\theta,\phi)\,\mathrm{d}\Omega = \frac{\epsilon_m \gamma n!(\mu+n)(\mu+n+1)}{(2\mu+2n+1)\Gamma(2\mu+n+1)}\delta_{\mu\mu'}\delta_{nn'} \tag{A.26}$$

$$\int_{\Omega_0} \bar{l}_q(\theta,\phi) \cdot \bar{l}_{q'}(\theta,\phi)\,\mathrm{d}\Omega = \frac{\epsilon_m \gamma n!(\mu+n)^2(\mu+n+1)^2}{(2\mu+2n+1)\Gamma(2\mu+n+1)}\delta_{\mu\mu'}\delta_{nn'} \tag{A.27}$$

$$\begin{aligned} \int_{\Omega_0} \bar{m}_q(\theta,\phi) \cdot \bar{n}_{q'}(\theta,\phi)\,\mathrm{d}\Omega &= \int_{\Omega_0} \bar{m}_q(\theta,\phi) \cdot \bar{l}_{q'}(\theta,\phi)\,\mathrm{d}\Omega \\ \int_{\Omega_0} \bar{n}_q(\theta,\phi) \cdot \bar{l}_{q'}(\theta,\phi)\,\mathrm{d}\Omega &= 0 \end{aligned} \tag{A.28}$$

where q and q' are the compact indices representing $\begin{smallmatrix} e \\ o \end{smallmatrix} \mu n$ and $\begin{smallmatrix} e \\ o \end{smallmatrix} \mu' n'$, respectively. $\delta_{q,q'}$ is the Kronecker delta defined as

$$\delta_{q,q'} = \begin{cases} 1 & \text{if } q = q', \\ 0 & \text{if } q \neq q', \end{cases} \tag{A.29}$$

and

$$\epsilon_m = \begin{cases} 2 & \text{if } m = 0, \\ 1 & \text{if } m \neq 0, \end{cases} \tag{A.30}$$

Using the orthogonality of the auxiliary functions, Orthogonality of the vector wave functions with superscript (1) over volume V bounded byS' are derived.

$$\int_V \bar{M}_q^{(1)}(k\bar{R}) \cdot \bar{M}_{q'}^{(1)}(k'\bar{R})dv = Q_{\mu n}(\mu+n)(\mu+n+1)\delta(k-k')\delta_{qq'}, \tag{A.31}$$

$$\int_V \bar{N}_q^{(1)}(k\bar{R}) \cdot \bar{N}_{q'}^{(1)}(k'\bar{R})dv = Q_{\mu n}(\mu+n)(\mu+n+1)\delta(k-k')\delta_{qq'} \tag{A.32}$$

and

$$\int_V \bar{M}_q^{(1)}(k\bar{R}) \cdot \bar{N}_{q'}^{(1)}(k'\bar{R})dv = 0 \tag{A.33}$$

$$Q_{\mu n} = \frac{\epsilon_m \pi \gamma n!}{2(2\mu+2n+1)\Gamma(2\mu+n+1)} \tag{A.34}$$